

ROBUST ALGEBRAIC MULTILEVEL PRECONDITIONING IN $H(\text{curl})$ AND $H(\text{div})$

S. K. TOMAR

ABSTRACT. An algebraic multilevel iteration method for solving system of linear algebraic equations arising in $H(\text{curl})$ and $H(\text{div})$ spaces are presented. The algorithm is developed for the discrete problem obtained by using the space of lowest order Nedelec and Raviart-Thomas-Nedelec elements. The theoretical analysis of the method is based only on some algebraic sequences and generalized eigenvalues of local (element-wise) problems. In the hierarchical basis framework, explicit recursion formulae are derived to compute the element matrices and the constant γ (which measures the quality of the space splitting) at any given level. It is proved that the proposed method is robust with respect to the problem parameters, and is of optimal order complexity. Supporting numerical results, including the case when the parameters have jumps, are also presented.

1. INTRODUCTION

Consider the finite element discretization of variational problems related to the bilinear form

$$(1.1) \quad \mathcal{A}(\mathbf{u}, \mathbf{v}) := \alpha(\mathbf{u}, \mathbf{v}) + \beta(\mathcal{X}\mathbf{u}, \mathcal{X}\mathbf{v}), \quad \alpha, \beta \in \mathbb{R}^+,$$

defined on the Hilbert space

$$(1.2) \quad H(\Omega, \mathcal{X}) := \{\mathbf{v} \in (L^2(\Omega))^d : \mathcal{X}\mathbf{v} \in L^2(\Omega)\}.$$

Here $\Omega \subset \mathbb{R}^d$, $d = 2, 3$, is a Lipschitz domain, and \mathcal{X} is the curl operator for $d = 2$ and div operator for $d = 3$. Note that $\text{div } \mathbf{v} = \partial_x v_1 + \partial_y v_2 + \partial_z v_3$ is the divergence of a three-dimensional vector $\mathbf{v} = [v_1, v_2, v_3]^T$, $\text{curl } \mathbf{v} = \partial_x v_2 - \partial_y v_1$ is the scalar curl of a two-dimensional vector $\mathbf{v} = [v_1, v_2]^T$, and (\cdot, \cdot) denotes the inner-product in $L^2(\Omega)$. For $\alpha = \beta = 1$, the bilinear form (1.1) is precisely the inner-product in $H(\Omega, \mathcal{X})$.

The adjoint of operator \mathcal{X} is defined by

$$\mathcal{X}^a = \begin{cases} \mathbf{curl} & \text{for } \mathcal{X} = \text{curl}, d = 2 \\ -\mathbf{grad} & \text{for } \mathcal{X} = \text{div}, d = 3 \end{cases},$$

where, for a scalar function w , $\mathbf{grad } w = [\partial_x w, \partial_y w, \partial_z w]^T$ (for three-dimensional problem), and $\mathbf{curl } w = [\partial_y w, -\partial_x w]^T$ (for two-dimensional problem). Associated with the inner-product \mathcal{A} , there exists a linear operator $\mathbf{A} := \alpha\mathbf{I} + \beta\mathcal{X}^a\mathcal{X}$, which maps $H(\Omega, \mathcal{X})$ onto its dual space, and is determined by the relation

$$(1.3) \quad (\mathbf{A}\mathbf{u}, \mathbf{v}) = \mathcal{A}(\mathbf{u}, \mathbf{v}), \quad \forall \mathbf{v} \in H(\Omega, \mathcal{X}),$$

Given a finite element space \mathcal{V}_h of $H(\Omega, \mathcal{X})$, the symmetric and positive-definite (SPD) operator $A_h : \mathcal{V}_h \rightarrow \mathcal{V}_h$, which is the discretization of the operator \mathbf{A} together with natural boundary conditions, is determined by

$$(1.4) \quad (A_h u_h, v_h) = \mathcal{A}(u_h, v_h), \quad \forall v_h \in \mathcal{V}_h.$$

The operator equation $\mathbf{A}\mathbf{u} = \mathbf{f}$, for $\mathbf{f} \in (L^2(\Omega))^d$, then leads to the following discrete problem

$$(1.5) \quad A_h u_h = f_h,$$

which is uniquely solvable. For $H(\Omega, \text{curl})$, such problems frequently occur in various contexts in electromagnetism, e.g., low-frequency time-harmonic Maxwell equations [33], or some formulations of the (Navier -) Stokes equations [18], and for $H(\Omega, \text{div})$ such problems frequently occur in, e.g., mixed formulations of elliptic problems, least-squares formulations of elliptic problems, part of fluid flow problems,

Date: June 5, 2018.

1991 Mathematics Subject Classification. 65N30, 65N22, 65N55.

Key words and phrases. Algebraic multilevel iteration method, lowest-order Nedelec and Raviart-Thomas-Nedelec spaces, optimal order complexity, $H(\text{div})$ and $H(\text{curl})$ spaces.

and in functional-type a posteriori error estimates, see, e.g., [2, 3, 30, 39, 40] and the reference therein. Therefore, developing fast solvers for large system of equations (1.5) is of significant importance.

Preconditioning methods for such linear systems in $H(\text{curl})$ within the framework of domain decomposition methods, multigrid methods, and auxiliary space methods have been proposed by several authors, see e.g., [2, 3, 19, 23, 43, 44] and the references therein. The first results for multigrid in $H(\text{div})$ (based on smoothing and approximation property) was presented in [13] for triangular elements. The first results for multigrid in $H(\text{curl})$ (within the framework of overlapping Schwarz methods) were obtained by Hiptmair in [20]. A unified treatment of multigrid methods for $H(\text{curl})$ and $H(\text{div})$ was presented by Hiptmair and Toselli in [21]. However, the condition number estimates of their preconditioned system were not robust with respect to the parameters α and β . Arnold et al. [3] employed the multigrid framework by developing necessary estimates for mixed finite element methods (FEM) based on discretizations of $H(\text{div})$ and $H(\text{curl})$, and thereby obtained parameter independent condition number estimates of the preconditioned system. Pasciak and Zhao studied the overlapping Schwarz methods for $H(\text{curl})$ in polyhedral domains in [37], and Reitzinger and Schoeberl studied algebraic multigrid methods for edge elements in [38]. Auxiliary space preconditioning, proposed by Xu in [46], was studied for $H_0(\Omega, \text{curl})$ (the space $H(\text{curl})$ with zero tangential trace) by Hiptmair et al. [22]. Nodal auxiliary space preconditioning in $H(\text{curl})$ and $H(\text{div})$ was studied by Hiptmair and Xu in [23], and the proposed preconditioner was robust with respect to the parameters α and β .

The main principles in constructing efficient multigrid and multilevel solvers for (1.5) are projections into spaces of divergence-free vector fields, see [44], or, alternatively, a discrete version of the Helmholtz decomposition, see e.g., [2], and/or the construction of a proper auxiliary space, see e.g., [23]. Moreover, an effective error reduction generally demands to complement the coarse-grid correction by an appropriate smoother, e.g., additive or multiplicative Schwarz smoother, cf. [3]. The simple scalar (point-wise) smoothers, in general, do not work satisfactorily for this class of problems. All of these methods may be viewed as subspace correction methods [45, 47], where different choices of specific components result in different methods (which also applies to the method presented in this paper).

Algebraic multilevel iteration (AMLI) methods were introduced by Axelsson and Vassilevski in a series of papers [7, 8, 9, 10]. The AMLI methods, which are recursive extensions of two-level methods for FEM [5], have been extensively analyzed in the context of conforming and nonconforming FEM (including discontinuous Galerkin methods), see [11, 12, 16, 24, 26, 27, 28, 34, 35, 36]. For a detailed systematic exposition of AMLI methods, see the monographs [25, 42]. These methods utilize a sequence of coarse-grid problems that are obtained from repeated application of a natural (and simple) hierarchical basis transformation, which is computationally advantageous. The underlying technique of these methods often requires only a few minor adjustments (mainly two-level hierarchical basis transformation) even if the underlying problem changes significantly. This is evident from the two different kind of problems considered in this paper, where the same algorithms (see Section 4) are used. Furthermore, the AMLI methods are robust with respect to the jumps in the operator coefficients (where classical multigrid methods suffer), and are computationally advantageous than classical algebraic multigrid methods.

In this paper, we first derive the results for two-dimensional $H(\text{curl})$ problem. Note that, in two-dimensions, the lowest-order Nedelec space can be obtained by a 90 degrees rotation of lowest-order Raviart-Thomas space. Therefore, the space splitting presented in [28] also applies in this case (and vice-versa). However, we present a unified treatment of the element matrices arising from (\mathbf{u}, \mathbf{v}) and $(\mathcal{X}\mathbf{u}, \mathcal{X}\mathbf{v})$, which helps in deriving the explicit recursion formulae in simpler forms and without any undetermined constants. Moreover, with the unified treatment we are able to extend the results to three-dimensional lowest-order Raviart-Thomas-Nedelec elements in a straight-forward manner. Our analysis is based only on some algebraic sequences and the generalized eigenvalues of local (element-wise) problems. In hierarchical setting, we derive explicit recursion formulae to compute the element matrices and the constant γ (which measures the quality of the space splitting) at any given level. The method is shown to be robust with respect to the parameters, i.e., the results hold uniformly for $0 < \alpha, \beta < \infty$.

The remainder of this paper is organized as follows. In Section 2 we briefly discuss the finite element discretization of the model problem (1.1) using the lowest-order Nedelec and Raviart-Thomas-Nedelec spaces. Section 3 starts with a brief description of the AMLI procedure (in Section 3.1). After presenting hierarchical basis transformations in Section 3.2, the construction of the hierarchical splitting of the lowest-order Nedelec and Raviart-Thomas-Nedelec spaces is presented in Section 3.3. In Section 3.4 a local two- and multi-level analysis is then presented and the main result is proved. The algorithms used

in this paper are provided in Section 4. Finally, in Section 5 we present numerical experiments. These include the cases with known analytical solution ($\alpha = \beta = 1$), fixing one of the parameters and varying other from 10^{-6} to 10^6 , and the case of jumping coefficients. The conclusions are drawn in Section 6.

2. FINITE ELEMENT DISCRETIZATION

In this section we briefly discuss the finite element discretization using lowest order Nedelec space in two-dimensions and lowest-order Raviart-Thomas-Nedelec space in three-dimensions, respectively.

2.1. Finite element discretization using Nedelec elements. We consider the tessellation of $\Omega \subset \mathbb{R}^2$ using square elements, and choose the reference element \hat{K} as $[-1, 1] \times [-1, 1]$. Let $P_{r_x, r_y}(\hat{K})$ denote the space of polynomials of degree $\leq r_x$ in x and $\leq r_y$ in y . Also, let $P_r(\partial\hat{K})$ denote the space of polynomials of degree $\leq r$ on $\partial\hat{K}$. For the construction of \mathcal{V}_h , we use the space of lowest-order edge elements (Nedelec space of first kind), which is denoted by \mathbf{N}^0 . The space $\mathbf{N}^0(\hat{K})$ is defined as

$$(2.1) \quad \mathbf{N}^0(\hat{K}) = P_{0,1}(\hat{K}) \times P_{1,0}(\hat{K}) = \left\{ \mathbf{v}(\hat{x}, \hat{y}) = \begin{bmatrix} v_1 + v_2 \hat{y} \\ v_3 + v_4 \hat{x} \end{bmatrix} \right\}.$$

Thus, the local basis for \mathbf{N}^0 has dimension 4. Moreover, for $\mathbf{v}_0 \in \mathbf{N}^0(\hat{K})$ we have

$$(2.2) \quad \text{curl } \mathbf{v}_0 \in P_{0,0}, \quad \mathbf{v}_0 \cdot \mathbf{t}|_{\partial\hat{K}} \in P_0(\partial\hat{K}),$$

where \mathbf{t} denotes the unit tangential vector to the element boundaries. For further details the reader is referred to, e.g., [33].

Now let $F : \hat{K} \rightarrow \mathbb{R}^2$ be a diffeomorphism of the reference element \hat{K} onto a physical element K , i.e., $K = F(\hat{K})$. By \mathcal{J} we denote the Jacobian matrix of the mapping, and by \mathcal{J}_D its determinant, which are defined as

$$\mathcal{J} = \begin{pmatrix} \partial_{\hat{x}} x & \partial_{\hat{y}} x \\ \partial_{\hat{x}} y & \partial_{\hat{y}} y \end{pmatrix}, \quad \mathcal{J}_D = |\det \mathcal{J}| = \partial_{\hat{x}} x \partial_{\hat{y}} y - \partial_{\hat{y}} x \partial_{\hat{x}} y > 0.$$

Then we have the following transformation relations:

$$(2.3) \quad \mathbf{w} = \mathcal{J}^{-T} \hat{\mathbf{w}}; \quad \text{curl } \mathbf{w} = \mathcal{J}_D^{-1} \text{curl } \hat{\mathbf{w}}, \quad \forall \mathbf{w} \in H(K, \text{curl}), \hat{\mathbf{w}} \in H(\hat{K}, \text{curl}).$$

The vector transformation $\mathbf{w} \rightarrow \mathcal{J}^{-T} \hat{\mathbf{w}}$ is called the covariant transformation, and $\text{curl } \mathbf{w} = \mathcal{J}_D^{-1} \text{curl } \hat{\mathbf{w}}$ is obtained via the well known Piola transformation $\mathbf{w} \rightarrow \mathcal{J}_D^{-1} \mathcal{J} \hat{\mathbf{w}}$.

We denote the element matrix for $\int_K \mathbf{u} \cdot \mathbf{v}$ by L_K , and for $\int_K \text{curl } \mathbf{u} \text{ curl } \mathbf{v}$ by C_K . For the \mathbf{N}^0 space based on uniform mesh composed of square elements, the element matrices L_K and C_K have the following structure

$$(2.4) \quad L_K = \frac{1}{6} \begin{bmatrix} 2 & 1 & 0 & 0 \\ 1 & 2 & 0 & 0 \\ 0 & 0 & 2 & 1 \\ 0 & 0 & 1 & 2 \end{bmatrix}, \quad C_K = \frac{1}{h^2} \begin{bmatrix} 1 & -1 & -1 & 1 \\ -1 & 1 & 1 & -1 \\ -1 & 1 & 1 & -1 \\ 1 & -1 & -1 & 1 \end{bmatrix}.$$

The overall element matrix $A_{K,C} := \alpha L_K + \beta C_K$, is thus given by

$$(2.5) \quad A_{K,C} = \frac{1}{6h^2} \begin{bmatrix} 2\alpha h^2 + 6\beta & \alpha h^2 - 6\beta & -6\beta & 6\beta \\ \alpha h^2 - 6\beta & 2\alpha h^2 + 6\beta & 6\beta & -6\beta \\ -6\beta & 6\beta & 2\alpha h^2 + 6\beta & \alpha h^2 - 6\beta \\ 6\beta & -6\beta & \alpha h^2 - 6\beta & 2\alpha h^2 + 6\beta \end{bmatrix}.$$

Letting $e = \kappa h^2$, with $\kappa = \alpha/\beta$, the element matrix can be written as

$$(2.6) \quad A_{K,C} = \frac{\beta}{6h^2} \begin{bmatrix} 2e + 6 & e - 6 & -6 & 6 \\ e - 6 & 2e + 6 & 6 & -6 \\ -6 & 6 & 2e + 6 & e - 6 \\ 6 & -6 & e - 6 & 2e + 6 \end{bmatrix}.$$

Clearly, for all $\alpha, \beta \in \mathbb{R}^+$, and thus $\kappa \in \mathbb{R}^+$, we have $e > 0$. Note that for fixed κ , and $h \rightarrow 0$, the element matrix $A_{K,C}$ is dominated by the matrix C_K (which has a non-zero kernel), whereas for moderate values of h it is a regular matrix. The near-nullspace of the matrix $A_{K,C}$ is given by the nullspace of the matrix C_K , which is associated with the local bilinear form $C_K(\mathbf{u}, \mathbf{v}) := (\text{curl } \mathbf{u}, \text{curl } \mathbf{v})_K$. As we shall see in the analysis, the proposed method is of optimal order for all $0 < \alpha, \beta < \infty$.

The following result can now be easily shown using [28, Lemma 2.1].

Lemma 2.1. (Near-nullspace of matrix $A_{K,C}$). *The element matrix $A_{K,C}$ given in (2.5) is symmetric positive definite (SPD). Moreover, the nullspace of the matrix C_K for a general element K with nodal coordinates (x_i, y_i) , $i \in \{1, 2, 3, 4\}$ is given by*

$$(2.7) \quad \ker(C_K) = \text{span}\{(1, 1, 0, 0)^T, (0, 0, 1, 1)^T, (x_1, x_2, y_3, y_4)^T\}.$$

Furthermore, in case of a uniform mesh composed of square N^0 elements, the matrix C_K is same for each element K and its nullspace is given by

$$\ker(C_K) = \text{span}\{(1, 1, 0, 0)^T, (0, 0, 1, 1)^T, (-1, 0, 0, 1)^T\}.$$

Remark 2.2. When using the lowest order Nedelec elements, the matrix C_K is always of rank one. In the global assembly this yields a matrix C whose rank equals the number of elements in the mesh. That is, the kernel of the global matrix C has dimension $\dim(\ker(C)) = n_E - n_K$, where n_E denotes the number of faces and n_K denotes the number of elements in the finite element mesh. Thereby, the dimension of the kernel is slightly more than half of the total number of degrees of freedom.

2.2. Finite element discretization using Raviart-Thomas-Nedelec elements. We consider the tessellation of $\Omega \subset \mathbb{R}^3$ using cubic elements, and choose the reference element \hat{K} as $[-1, 1]^3$. Let $P_{r_x, r_y, r_z}(\hat{K})$ denote the space of polynomials of degree $\leq r_x$ in x , $\leq r_y$ in y and $\leq r_z$ in z , respectively. Also, let $P_{r_1, r_2}(\partial\hat{K})$ denote the space of polynomials of degrees $\leq r_1$ and $\leq r_2$ in the respective dimensions on $\partial\hat{K}$. For the construction of \mathcal{V}_h , we use the space of lowest-order Raviart-Thomas-Nedelec elements, which is denoted by RTN^0 . The space $\text{RTN}^0(\hat{K})$ is defined as

$$(2.8) \quad \text{RTN}^0(\hat{K}) = P_{1,0,0}(\hat{K}) \times P_{0,1,0}(\hat{K}) \times P_{0,0,1}(\hat{K}) = \left\{ \mathbf{v}(\hat{x}, \hat{y}, \hat{z}) = \begin{bmatrix} v_1 + v_2 \hat{x} \\ v_3 + v_4 \hat{y} \\ v_5 + v_6 \hat{z} \end{bmatrix} \right\}.$$

Thus, the local basis for RTN^0 has dimension 6. Moreover, for $\mathbf{v}_0 \in \text{RTN}^0(\hat{K})$ we have

$$(2.9) \quad \text{div } \mathbf{v}_0 \in P_{0,0,0}, \quad \mathbf{v}_0 \cdot \mathbf{n}|_{\partial\hat{K}} \in P_{0,0}(\partial\hat{K}),$$

where \mathbf{n} denotes the unit normal vector to the element faces. For further details the reader is referred to, e.g., [14].

Now let $F : \hat{K} \rightarrow \mathbb{R}^3$ be a diffeomorphism of the reference element \hat{K} onto a physical element K , i.e., $K = F(\hat{K})$. By \mathcal{J} we denote the Jacobian matrix of the mapping, and by \mathcal{J}_D its determinant, which are defined as

$$\mathcal{J} = \begin{pmatrix} \partial_{\hat{x}}x & \partial_{\hat{y}}x & \partial_{\hat{z}}x \\ \partial_{\hat{x}}y & \partial_{\hat{y}}y & \partial_{\hat{z}}y \\ \partial_{\hat{x}}z & \partial_{\hat{y}}z & \partial_{\hat{z}}z \end{pmatrix}, \quad \mathcal{J}_D = |\det \mathcal{J}| > 0.$$

Then we have the following relations:

$$(2.10) \quad \mathbf{w} = \mathcal{J}_D^{-1} \mathcal{J} \hat{\mathbf{w}}; \quad \text{div } \mathbf{w} = \mathcal{J}_D^{-1} \text{div } \hat{\mathbf{w}}, \quad \forall \mathbf{w} \in H(K, \text{div}), \hat{\mathbf{w}} \in H(\hat{K}, \text{div}),$$

by the well known Piola transformation, see e.g., [14].

We denote the element matrix for $\int_K \mathbf{u} \cdot \mathbf{v}$ by L_K , and for $\int_K \text{div } \mathbf{u} \text{ div } \mathbf{v}$ by D_K . For the RTN^0 space based on uniform mesh composed of cubic elements, the element matrices L_K and D_K have the following structure

$$(2.11) \quad L_K = \frac{1}{6h} \begin{bmatrix} 2 & 1 & 0 & 0 & 0 & 0 \\ 1 & 2 & 0 & 0 & 0 & 0 \\ 0 & 0 & 2 & 1 & 0 & 0 \\ 0 & 0 & 1 & 2 & 0 & 0 \\ 0 & 0 & 0 & 0 & 2 & 1 \\ 0 & 0 & 0 & 0 & 1 & 2 \end{bmatrix}, \quad D_K = \frac{1}{h^3} \begin{bmatrix} 1 & -1 & 1 & -1 & 1 & -1 \\ -1 & 1 & -1 & 1 & -1 & 1 \\ 1 & -1 & 1 & -1 & 1 & -1 \\ -1 & 1 & -1 & 1 & -1 & 1 \\ 1 & -1 & 1 & -1 & 1 & -1 \\ -1 & 1 & -1 & 1 & -1 & 1 \end{bmatrix}.$$

The overall element matrix $A_{K,D} := \alpha L_K + \beta D_K$, is thus given by

$$(2.12) \quad A_{K,D} = \frac{1}{6h^3} \begin{bmatrix} 2\alpha h^2 + 6\beta & \alpha h^2 - 6\beta & 6\beta & -6\beta & 6\beta & -6\beta \\ \alpha h^2 - 6\beta & 2\alpha h^2 + 6\beta & -6\beta & 6\beta & -6\beta & 6\beta \\ 6\beta & -6\beta & 2\alpha h^2 + 6\beta & \alpha h^2 - 6\beta & 6\beta & -6\beta \\ -6\beta & 6\beta & \alpha h^2 - 6\beta & 2\alpha h^2 + 6\beta & -6\beta & 6\beta \\ 6\beta & -6\beta & 6\beta & -6\beta & 2\alpha h^2 + 6\beta & \alpha h^2 - 6\beta \\ -6\beta & 6\beta & -6\beta & 6\beta & \alpha h^2 - 6\beta & 2\alpha h^2 + 6\beta \end{bmatrix}.$$

With the definition of e introduced before (2.6), the element matrix can be written as

$$(2.13) \quad A_{K,D} = \frac{\beta}{6h^3} \begin{bmatrix} 2e + 6 & e - 6 & 6 & -6 & 6 & -6 \\ e - 6 & 2e + 6 & -6 & 6 & -6 & 6 \\ 6 & -6 & 2e + 6 & e - 6 & 6 & -6 \\ -6 & 6 & e - 6 & 2e + 6 & -6 & 6 \\ 6 & -6 & 6 & -6 & 2e + 6 & e - 6 \\ -6 & 6 & -6 & 6 & e - 6 & 2e + 6 \end{bmatrix}.$$

Note again that for fixed κ , and $h \rightarrow 0$, the element matrix $A_{K,D}$ is dominated by the matrix D_K (which has a non-zero kernel), whereas for moderate values of h it is a regular matrix. The near-nullspace of the matrix $A_{K,D}$ is given by the nullspace of the matrix D_K , which is associated with the local bilinear form $\mathcal{D}_K(\mathbf{u}, \mathbf{v}) := (\text{div } \mathbf{u}, \text{div } \mathbf{v})_K$. As we shall see in the analysis, the proposed method is of optimal order for all $0 < \alpha, \beta < \infty$.

Proposition 2.3. (Near-nullspace of matrix $A_{K,D}$). *The element matrix $A_{K,D}$ given in (2.12) is symmetric positive definite (SPD). Furthermore, in case of a uniform mesh composed of cubic RTN⁰ elements, the matrix D_K is same for each element K and its nullspace is given by*

$$\begin{aligned} & \ker(D_K) \\ &= \text{span}\{(1, 1, 0, 0, 0, 0)^T, (-1, 0, 1, 0, 0, 0)^T, (1, 0, 0, 1, 0, 0)^T, (-1, 0, 0, 0, 1, 0)^T, (1, 0, 0, 0, 0, 1)^T\}. \end{aligned}$$

Proof. Since the coefficients α and β in (2.12) are positive, it follows from equation (1.5) that $A_{K,D}$ is SPD for a general element K . Moreover, for a uniform mesh composed of cubic RTN⁰ elements, since the vector $(1, -1, 1, -1, 1, -1)^T$ is orthogonal to the kernel of D_K , it is clear that the rank-one matrix D_K is of the form $c \cdot (1, -1, 1, -1, 1, -1)^T \cdot (1, -1, 1, -1, 1, -1)$, for some constant c . \square

Remark 2.4. When using the lowest order Raviart-Thomas-Nedelec elements, the matrix D_K is always of rank one. In the global assembly this yields a matrix D whose rank equals the number of elements in the mesh. That is, the kernel of the global matrix D has dimension $\dim(\ker(D)) = n_F - n_K$, where n_F denotes the number of faces and n_K denotes the number of elements in the finite element mesh. Thereby, the dimension of the kernel is slightly more than two-third of the total number of degrees of freedom.

3. ALGEBRAIC MULTILEVEL ITERATION

For the solution of the linear system arising from (1.5), we describe and analyze the AMLI method in the remainder of this section. Our presentation follows [28].

3.1. The AMLI procedure. In what follows we will denote by $M^{(\ell)}$ a preconditioner for a finite element (stiffness) matrix $A^{(\ell)}$ corresponding to a ℓ times refined mesh ($0 \leq \ell \leq L$). We will also make use of the corresponding ℓ^{th} level hierarchical matrix $\hat{A}^{(\ell)}$, which is related to $A^{(\ell)}$ via a two-level hierarchical basis (HB) transformation $J^{(\ell)}$, i.e.,

$$(3.1) \quad \hat{A}^{(\ell)} = J^{(\ell)} A^{(\ell)} (J^{(\ell)})^T.$$

The transformation matrix $J^{(\ell)}$ specifies the space splitting, and will be described in detail in Section 3.2. By $A_{ij}^{(\ell)}$ and $\hat{A}_{ij}^{(\ell)}$, $1 \leq i, j \leq 2$, we denote the blocks of $A^{(\ell)}$ and $\hat{A}^{(\ell)}$ that correspond to the fine-coarse partitioning of degrees of freedom (DOF) where the DOF associated with the coarse mesh are numbered last.

The aim is to build a multilevel preconditioner $M^{(L)}$ for the coefficient matrix $A^{(L)} := A_h$ at the level of the finest mesh that has a uniformly bounded (relative) condition number

$$\kappa(M^{(L)-1} A^{(L)}) = \mathcal{O}(1),$$

and an optimal computational complexity, that is, linear in the number of degrees of freedom N_L at the finest mesh (grid). In order to achieve this goal hierarchical basis methods can be combined with various types of stabilization techniques. One particular purely algebraic stabilization technique is the so-called Algebraic Multi-Level Iteration (AMLI) method, which is presented below.

We have the following two-level hierarchical basis representation at level ℓ

$$(3.2) \quad \hat{A}^{(\ell)} = \begin{bmatrix} \hat{A}_{11}^{(\ell)} & \hat{A}_{12}^{(\ell)} \\ \hat{A}_{21}^{(\ell)} & \hat{A}_{22}^{(\ell)} \end{bmatrix} = \begin{bmatrix} \hat{A}_{11}^{(\ell)} & \hat{A}_{12}^{(\ell)} \\ \hat{A}_{21}^{(\ell)} & A^{(\ell-1)} \end{bmatrix}.$$

Starting at level 0 (associated with the coarsest mesh), on which a complete LU factorization of the matrix $A^{(0)}$ is performed, we define

$$(3.3) \quad M^{(0)} := A^{(0)}.$$

Given the preconditioner $M^{(\ell-1)}$ at level $\ell - 1$, the preconditioner $M^{(\ell)}$ at level ℓ is then defined by

$$(3.4) \quad M^{(\ell)} := L^{(\ell)} U^{(\ell)},$$

where

$$(3.5) \quad L^{(\ell)} := \begin{bmatrix} C_{11}^{(\ell)} & 0 \\ \hat{A}_{21}^{(\ell)} & C_{22}^{(\ell)} \end{bmatrix}, \quad U^{(\ell)} := \begin{bmatrix} I & C_{11}^{(\ell)-1} \hat{A}_{12}^{(\ell)} \\ 0 & I \end{bmatrix}.$$

Here $C_{11}^{(\ell)}$ is a preconditioner for the pivot block $A_{11}^{(\ell)}$, and

$$(3.6) \quad C_{22}^{(\ell)} := A^{(\ell-1)} \left(I - p^{(\ell)}(M^{(\ell-1)-1} A^{(\ell-1)}) \right)^{-1}$$

is an approximation to the Schur complement $S = A^{(\ell-1)} - \hat{A}_{21}^{(\ell)} C_{11}^{(\ell)-1} \hat{A}_{12}^{(\ell)}$, where $A^{(\ell-1)} = \hat{A}_{22}^{(\ell)}$ is the stiffness matrix at the coarse level $\ell - 1$, and $p^{(\ell)}$ is a certain stabilization polynomial of degree ν_ℓ satisfying the condition

$$(3.7) \quad 0 \leq p^{(\ell)}(x) < 1, \quad \forall 0 < x \leq 1, \quad \text{and } p^{(\ell)}(0) = 1.$$

It is easily seen that (3.6) is equivalent to

$$(3.8) \quad C_{22}^{(\ell)-1} = M^{(\ell-1)-1} q^{(\ell)}(A^{(\ell-1)} M^{(\ell-1)-1}),$$

where the polynomial $q^{(\ell)}(x)$ is given by

$$(3.9) \quad q^{(\ell)}(x) = \frac{1 - p^{(\ell)}(x)}{x}.$$

We note that the multilevel preconditioner defined via (3.4) is getting close to a two-level method when $q^{(\ell)}(x)$ closely approximates $1/x$, in which case $C_{22}^{(\ell)-1} \approx A^{(\ell-1)-1}$. In order to construct an efficient multilevel method the action of $C_{22}^{(\ell)-1}$ on an arbitrary vector should be much cheaper to compute (in terms of the number of arithmetic operations) than the action of $A^{(\ell-1)-1}$. Optimal order solution algorithms typically require that the arithmetic work for one application of $C_{22}^{(\ell)-1}$ is of the order $\mathcal{O}(N_{\ell-1})$ where $N_{\ell-1}$ denotes the number of unknowns at level $\ell - 1$.

To reduce the overall complexity of AMLI methods (to achieve optimal computational complexity), various stabilization techniques can be used. It is well known from the theory introduced in [7, 8] that a properly shifted and scaled Chebyshev polynomial $p^{(\ell)} := p_{\nu_\ell}$ of degree ν_ℓ can be used to stabilize the condition number of $M^{(\ell)-1} A^{(\ell)}$ (and thus obtain optimal order computational complexity). Other polynomials such as the best polynomial approximation of $1/x$ in uniform norm also qualify for stabilization, see, e.g., [29]. This approach requires the computation of polynomial coefficients which depends on the bounds of the eigenvalues of the preconditioned system. Alternatively, a few inner flexible conjugate gradient (FCG) type iterations are performed at coarse levels to stabilize (or freeze the residual reduction factor of) the outer FCG iteration, which lead to parameter-free AMLI methods [9, 10, 24, 34, 35, 36]. In general, the resulting nonlinear (variable step) multilevel preconditioning method is almost equally efficient as linear AMLI method, and, because its realization does not rely on any spectral bounds, it is

easier to implement than the linear AMLI method (based on a stabilization polynomial). For a convergence analysis of nonlinear AMLI see, e.g., [24, 25, 42].

Typically, the iterative solution process is of optimal order of computational complexity if the degree $\nu_\ell = \nu$ of the matrix polynomial (or alternatively, the number of inner iterations for nonlinear AMLI) at level ℓ satisfies the optimality condition

$$(3.10) \quad 1/\sqrt{(1-\gamma^2)} < \nu < \tau,$$

where $\tau \approx \tau_\ell = N_\ell/N_{\ell-1}$ denotes the reduction factor of the number of degrees of freedom (DOF), and γ denotes the constant in the strengthened Cauchy-Bunyakowski-Schwarz (CBS) inequality. In case of standard (full) coarsening, the value of τ is approximately 4 for the sequence of N^0 spaces, and 8 for the sequence of RTN^0 spaces. These sequences will be constructed in the next subsections. For a more detailed discussion of AMLI methods, including implementation issues see, e.g., [25, 42].

Remark 3.1. The commonly used AMLI algorithm was originally introduced and studied in a multiplicative form (3.4), see [7, 8]. However, the preconditioner can also be constructed in the additive form, which is defined as follows [4, 6, 25]

$$(3.11) \quad M_A^{(\ell)} := \begin{bmatrix} C_{11}^{(\ell)} & 0 \\ 0 & C_{22}^{(\ell)} \end{bmatrix}.$$

In this case the optimal order of computational complexity demands that the matrix polynomial degree (or the number of inner iterations of nonlinear AMLI) satisfy the following relation

$$(3.12) \quad \sqrt{(1+\gamma)/(1-\gamma)} < \nu < \tau.$$

3.2. Hierarchical basis for \mathcal{V}_h . The AMLI methods we are considering here, for the solution of (1.5), are based on a proper splitting of the space \mathcal{V}_h .

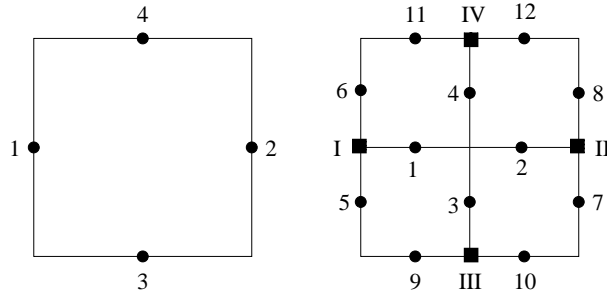


FIGURE 1. Macro-element obtained after one regular mesh-refinement step

For N^0 subspace of $H(\text{curl})$, the particular two-level HB transformation that induces this splitting was introduced in the context of linear nonconforming Crouzeix-Raviart (CR) elements in [11, 12]. It was later studied for quadrilateral rotated bilinear (Rannacher-Turek) type elements in [16]. Note that the similarities of the HB transformation when using CR elements and Nedelec elements is due to the algebraic nature of the problem. For the discretization based on linear elements (for meshes consisting of triangles) or bilinear elements (for meshes consisting of squares), similar HB transformation matrix can be used. However, suitable changes will be required when working with meshes consisting of general quadrilaterals.

Consider two consecutive discretizations \mathcal{T}_H (coarse level) and \mathcal{T}_h (fine level). Figure 1 illustrates a macro-element G (at fine level) obtained from a coarse element by one regular mesh-refinement step. Let $\varphi_G = \{\phi_i(x, y)\}_{i=1}^{12}$ be the macro-element vector of the nodal basis functions. Using the local numbering of DOF, as shown in Figure 1 (right picture), a macro-element level (local) transformation matrix J_G is constructed based on differences and aggregates of each pair of basis functions ϕ_i and ϕ_j that correspond

macro-element G (at fine level) obtained from a coarse element by one regular mesh-refinement step. The colors green, magenta and blue represent the face directions and face DOFs for x , y and z directions, respectively. Let $\varphi_G = \{\phi_i(x, y)\}_{i=1}^{36}$ be the macro-element vector of the nodal basis functions. Using the local numbering of DOF, as shown in Figure 2 (second, third and fourth row of pictures), a macro-element level (local) transformation matrix J_G is constructed based on differences and aggregates of basis functions ϕ_i and ϕ_j that correspond to a macro element face, i.e.,

$$(3.14a) \quad J_G = \frac{1}{4} \begin{bmatrix} 4I & \\ & J_{G;22} \end{bmatrix},$$

where I is the 12×12 identity matrix and

$$(3.14b) \quad J_{G;22} = \begin{bmatrix} P_D & & & & & \\ & P_D & & & & \\ & & P_D & & & \\ & & & P_D & & \\ & & & & P_D & \\ & & & & & P_D \\ P_A^1 & P_A^2 & P_A^3 & P_A^4 & P_A^5 & P_A^6 \end{bmatrix}.$$

Here each block P_A^i , $i = 1, 2, \dots, 6$, which reflects the basis functions obtained by aggregates, is a 6×4 matrix with all zeros except i^{th} -row which has all ones. The block P_D , which reflects the orthogonal transformation to aggregates, and obtained by suitable combination of differences, is given by

$$(3.14c) \quad P_D = \begin{bmatrix} 1 & -1 & 1 & -1 \\ 1 & 1 & -1 & -1 \\ 1 & -1 & -1 & 1 \end{bmatrix}.$$

The transformations (3.13)-(3.14) define a two-level hierarchical basis $\hat{\varphi}_G$ locally, namely, $\hat{\varphi}_G = J_G \varphi_G$.

3.3. Hierarchical splitting. Let A_G be the macro-element stiffness matrix corresponding to $G \in \mathcal{T} = \mathcal{T}_h$. The global stiffness matrix A_h can be written as

$$A_h = \sum_{G \in \mathcal{T}} R_G^T A_G R_G,$$

where R_G denotes the natural inclusion (canonical injection) of the matrix A_G for all G in \mathcal{T} . Note that the matrix A_G is of size 12×12 for two-dimensional $H(\text{curl})$ problem, and of size 36×36 for three-dimensional $H(\text{div})$ problem. Then the hierarchical two-level macro-element matrix is given by

$$\hat{A}_G = J_G A_G J_G^T,$$

and the related global two-level matrix can be obtained via assembling, i.e., $\hat{A}_h = \sum_{G \in \mathcal{T}} R_G^T \hat{A}_G R_G$. Alternatively, one can compute the matrix \hat{A}_h via the triple matrix product

$$(3.15) \quad \hat{A}_h = J A_h J^T,$$

where the global transformation matrix J is induced by the local transformations, i.e.,

$$J|_G = J_G, \quad \forall G \in \mathcal{T}.$$

In other words, global and local transformations are compatible in the sense that restricting J to the DOF of any macro-element G we obtain J_G . Now, if we number those DOF that correspond to interior nodes of the macro elements first, the global two-level stiffness matrix \hat{A}_h has the 2×2 block structure

$$(3.16) \quad \hat{A}_h = \begin{bmatrix} \hat{A}_{11} & \hat{A}_{12} \\ \hat{A}_{21} & \hat{A}_{22} \end{bmatrix},$$

where \hat{A}_{11} corresponds to the *interior unknowns*. We follow the *first reduce* (FR) approach, see e.g., [11, 12, 16, 17], where these interior unknowns are first eliminated *exactly*. This static condensation step can be written in the form

$$(3.17) \quad \hat{A}_h = \begin{bmatrix} \hat{A}_{11} & 0 \\ \hat{A}_{21} & B \end{bmatrix} \begin{bmatrix} I_1 & \hat{A}_{11}^{-1} \hat{A}_{12} \\ 0 & I_2 \end{bmatrix},$$

with the Schur complement $B = \hat{A}_{22} - \hat{A}_{21}\hat{A}_{11}^{-1}\hat{A}_{12}$. Next, the matrix B is partitioned into 2×2 blocks, i.e.,

$$(3.18) \quad B = \begin{bmatrix} B_{11} & B_{12} \\ B_{21} & B_{22} \end{bmatrix},$$

where B_{11} and B_{22} correspond to the *differences* and *aggregates* of basis functions (associated with one macro-element edge or face), respectively. The matrix B_{22} at level ℓ then defines the coarse-grid matrix $A^{(\ell-1)}$ in the AMLI hierarchy, cf. (3.2). This algorithm can be applied recursively on each level $\ell = L, L-1, \dots, 1$. The resulting algorithm is then of optimal computational complexity, see e.g., [28, Remark 3.1].

3.4. Local analysis. In the two-level framework we denote by \mathcal{V}_1 and \mathcal{V}_2 the subspaces of the finite element space \mathcal{V}_h . The space \mathcal{V}_2 is spanned by the coarse-space basis functions (aggregates) and \mathcal{V}_1 is the complement of \mathcal{V}_2 in \mathcal{V}_h , i.e., \mathcal{V}_h is a direct sum of \mathcal{V}_1 and \mathcal{V}_2 :

$$(3.19) \quad \mathcal{V}_h = \mathcal{V}_1 \oplus \mathcal{V}_2.$$

A measure for the quality of this splitting is the constant γ in the strengthened CBS inequality, which is defined by the relation

$$\gamma = \cos(\mathcal{V}_1, \mathcal{V}_2) := \sup_{\mathbf{u} \in \mathcal{V}_1, \mathbf{v} \in \mathcal{V}_2} \frac{\mathcal{A}(\mathbf{u}, \mathbf{v})}{\sqrt{\mathcal{A}(\mathbf{u}, \mathbf{u})\mathcal{A}(\mathbf{v}, \mathbf{v})}}.$$

It is well known (see, e.g., [5]) that γ can be estimated locally over each macro element G , and that $\gamma = \max_G \gamma_G$, where

$$\gamma_G := \sup_{\mathbf{u} \in \mathcal{V}_1(G), \mathbf{v} \in \mathcal{V}_2(G)} \frac{\mathcal{A}_G(\mathbf{u}, \mathbf{v})}{\sqrt{\mathcal{A}_G(\mathbf{u}, \mathbf{u})\mathcal{A}_G(\mathbf{v}, \mathbf{v})}}.$$

The spaces $\mathcal{V}_1(G)$, $\mathcal{V}_2(G)$, and the bilinear form $\mathcal{A}_G(\mathbf{u}, \mathbf{v})$ correspond to the restriction of \mathcal{V}_1 , \mathcal{V}_2 , and $\mathcal{A}(\mathbf{u}, \mathbf{v})$, respectively, to the macro element G .

We perform this local analysis on the matrix level, where the splitting (3.19) is obtained via the two-level hierarchical basis transformation described in Section 3.2, and the space \mathcal{V}_h corresponds to the choice of lowest order Nedgelec or Raviart-Thomas-Nedgelec elements. In this setting the upper left block of \hat{A}_h is block-diagonal. Note that, for two-dimensional $H(\text{curl})$ problem, the diagonal blocks of \hat{A}_{11} are of size 4×4 , which can be associated with the interior nodes $\{1, 2, \dots, 4\}$ in the right picture of Figure 1, and for three-dimensional $H(\text{div})$ problem, the diagonal blocks of \hat{A}_{11} are of size 12×12 , which can be associated with the interior nodes $\{1, 2, \dots, 12\}$ in the center column of second, third and fourth row of pictures in Figure 2. Therefore, we first compute the local Schur complements arising from static condensation of the interior DOF and obtain the matrices B_G . Next we split each matrix B_G as

$$B_G = \left[\begin{array}{cc} B_{G,11} & B_{G,12} \\ B_{G,21} & B_{G,22} \end{array} \right] \begin{array}{l} \} \text{differences} \\ \} \text{aggregates} \end{array},$$

written again in two-by-two block form. For two-dimensional $H(\text{curl})$ problem, the block $B_{G,11}$ and $B_{G,22}$ are both of size 4×4 , and for three-dimensional $H(\text{div})$ problem the block $B_{G,11}$ is of size 18×18 and the block $B_{G,22}$ is of size 6×6 . We have thus reduced the problem of estimating the CBS constant of the splitting (3.19) to a small-sized local problem that involves the matrix B_G . Following the general theory, see [5, 15], to estimate the CBS constant γ , it suffices to compute the minimal eigenvalue of the generalized eigenproblem

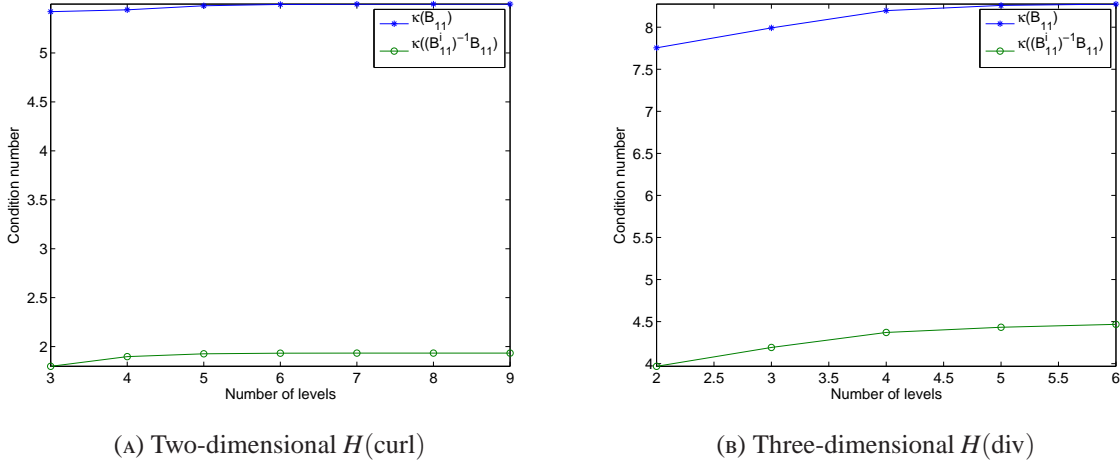
$$(3.20) \quad S_G \mathbf{v}_G = \lambda_{G,\min} B_{G,22} \mathbf{v}_G, \quad \forall \mathbf{v}_G,$$

where $S_G = B_{G,22} - B_{G,21} B_{G,11}^{-1} B_{G,12}$. The CBS constant γ can then be estimated as follows

$$(3.21) \quad \gamma^2 \leq \max_{G \in \mathcal{T}} \gamma_G^2 = \max_{G \in \mathcal{T}} (1 - \lambda_{G,\min}).$$

Note that the matrix $B_{G,11}$ is a well conditioned matrix, see Figure 3, and therefore, it can be inverted cheaply, either by an iterative process or by, for example, an incomplete LU factorization [41], which is denoted by B_{11}^i in Figure 3.

We now first prove some auxiliary (stand-alone) results on algebraic sequences, which we will use to bound the CBS constant γ .

FIGURE 3. Condition number of the matrix $B_{G,11}$

Lemma 3.2. For all $e > 0$, consider the coupled sequences

$$(3.22a) \quad b_0 = e - 6, \quad a_0 = 2e + 6 = 2(b_0 + 9),$$

$$(3.22b) \quad b_{\ell+1} = -b_\ell^2/a_\ell, \quad a_{\ell+1} = 2a_\ell + b_{\ell+1}, \quad \ell = 0, 1, 2, \dots$$

Let $r_\ell = b_\ell/a_\ell$. Then we have

$$(3.23a) \quad b_{\ell+1}/a_\ell = -r_\ell^2, \quad a_{\ell+1}/a_\ell = 2 - r_\ell^2, \quad r_{\ell+1} = -r_\ell^2/(2 - r_\ell^2),$$

$$(3.23b) \quad a_{\ell+1} - b_{\ell+1} = 2a_\ell, \quad a_{\ell+1} + b_{\ell+1} = \frac{2}{a_\ell}(a_\ell^2 - b_\ell^2) = 2a_\ell(1 - r_\ell^2), \quad \frac{a_{\ell+1} + b_{\ell+1}}{a_{\ell+1} - b_{\ell+1}} = 1 - r_\ell^2.$$

Moreover, the following bound holds

$$(3.24a) \quad -1 < r_0 < 1/2, \text{ and } -1 < r_\ell \leq 0 \quad \forall \ell = 1, 2, \dots,$$

$$(3.24b) \quad a_\ell > \dots a_1 > a_0 > 6, \quad 0 \leq r_\ell^2 \leq \dots \leq r_1^2 \leq r_0^2 < 1, \forall \ell = 0, 1, 2, \dots$$

Proof. Using the definition of r_ℓ in (3.22b), we get $b_{\ell+1}/a_\ell = -r_\ell^2$, and thus $a_{\ell+1}/a_\ell = 2 - r_\ell^2$. The last relation of (3.23a) then immediately follows. The relations (3.23b) are also easily obtained from (3.22b) and (3.23a).

Clearly, for $e > 0$, we have $a_0 > 6$, and since $r_0 = b_0/a_0 = (e - 6)/(2e + 6)$, it is easy to see that $-1 < r_0 < 1/2$. The latter also implies that $0 \leq r_0^2 < 1$. We now prove the remaining bounds using induction.

$\ell = 0$. Since $a_1/a_0 = 2 - r_0^2 > 1$, we have $a_1 > a_0 > 6$. Moreover, $r_1 = -r_0^2/(2 - r_0^2)$. This implies that $-1 < r_1 \leq 0$, and thus $0 \leq r_1^2 < 1$. Furthermore, when $r_0 \neq 0$, we have

$$r_1^2 = \left(\frac{-r_0^2}{2 - r_0^2} \right)^2 \Rightarrow \frac{r_1^2}{r_0^2} = \frac{r_0^2}{(2 - r_0^2)^2} < 1.$$

And, since $r_1 = 0$ if $r_0 = 0$, we have $r_1^2 \leq r_0^2 < 1$.

$\ell = n$. Assume that the relations (3.24) hold for $\ell = n$. Since $a_{n+1}/a_n = 2 - r_n^2 > 1$, we have $a_{n+1} > a_n > 6$. Moreover, $r_{n+1} = -r_n^2/(2 - r_n^2)$. This implies that $-1 < r_{n+1} \leq 0$, and thus $0 \leq r_{n+1}^2 < 1$. Also, when $r_n \neq 0$, we have

$$r_{n+1}^2 = \left(\frac{-r_n^2}{2 - r_n^2} \right)^2 \Rightarrow \frac{r_{n+1}^2}{r_n^2} = \frac{r_n^2}{(2 - r_n^2)^2} < 1.$$

And, since $r_{n+1} = 0$ if $r_n = 0$, we have $r_{n+1}^2 \leq r_n^2 < 1$.

This concludes the proof. \square

Lemma 3.3. Let $e > 0$ and the sequences a_ℓ and b_ℓ be as defined in Lemma 3.2. Then for

$$(3.25) \quad c_{\ell,C}^2 = \frac{36(a_\ell + b_\ell)}{(a_\ell^2 - 36)(a_\ell - b_\ell)},$$

the following bounds hold for all $\ell = 0, 1, 2, \dots$

$$(3.26) \quad c_{\ell,C}^2 < c_{\ell-1,C}^2 < \dots < c_{1,C}^2 < c_{0,C}^2 < 3/8.$$

Proof. From $a_0 = 2e + 6$ and $b_0 = e - 6$, we have $a_0 - b_0 = e + 12$, $a_0 + b_0 = 3e$, $a_0 - 6 = 2e$, and $a_0 + 6 = 2(e + 6)$. Substituting these relations in the definition of $c_{0,C}^2$, we get

$$(3.27) \quad c_{0,C}^2 = \frac{27}{(e + 6)(e + 12)} < 3/8.$$

Now

$$c_{1,C}^2 - c_{0,C}^2 = \frac{36((a_1 + b_1)(a_0^2 - 36)(a_0 - b_0) - (a_0 + b_0)(a_1^2 - 36)(a_1 - b_1))}{(a_1^2 - 36)(a_1 - b_1)(a_0^2 - 36)(a_0 - b_0)}.$$

Substituting the values of a_0, a_1, b_0 and b_1 , and after some lengthy, but simple calculations, we find that

$$c_{1,C}^2 - c_{0,C}^2 = \frac{108e(-9e^2(312 + 80e + 5e^2))}{(e + 3)(a_1^2 - 36)(a_1 - b_1)(a_0^2 - 36)(a_0 - b_0)}.$$

Since the denominator is a positive quantity, we get $c_{1,C}^2 - c_{0,C}^2 < 0$, and thus

$$(3.28) \quad c_{1,C}^2 < 3/8.$$

For remaining bounds, we again use induction. Note that, using (3.23b) we get

$$(3.29) \quad c_{\ell+1,C}^2 = \frac{36(a_{\ell+1} + b_{\ell+1})}{(a_{\ell+1}^2 - 36)(a_{\ell+1} - b_{\ell+1})} = \frac{36(1 - r_\ell^2)}{(a_{\ell+1}^2 - 36)}.$$

Therefore, to show that $c_{\ell+1,C}^2 < 3/8$, it suffices to show that

$$(3.30) \quad a_{\ell+1}^2 - 36 > 96(1 - r_\ell^2).$$

Since $c_{1,C}^2 < 3/8$, we clearly have $a_1^2 - 36 > 96(1 - r_0^2)$. Now assume that the relation (3.30) holds for $\ell = n - 1$, i.e.,

$$(3.31) \quad a_n^2 - 36 > 96(1 - r_{n-1}^2).$$

Multiplying (3.31) by $(2 - r_n^2)^2$ and subtracting 36 from both sides we get

$$\begin{aligned} (2 - r_n^2)^2 a_n^2 - 36 &> 36(2 - r_n^2)^2 + 96(1 - r_{n-1}^2)(2 - r_n^2)^2 - 36 \\ \Rightarrow a_{n+1}^2 - 36 &> 96((2 - r_n^2)^2(11/8 - r_{n-1}^2) - 3/8). \end{aligned}$$

We need to show that $(2 - r_n^2)^2(11/8 - r_{n-1}^2) - 3/8 > 1 - r_n^2$, i.e.,

$$(3.32) \quad g_n := (2 - r_n^2)^2(11/8 - r_{n-1}^2) + r_n^2 - 11/8 > 0.$$

From the recurrence relation on r_n from (3.23a), we have

$$r_n^2 = \frac{r_{n-1}^4}{(2 - r_{n-1}^2)^2}, \quad 2 - r_n^2 = \frac{(r_{n-1}^4 - 8r_{n-1}^2 + 8)}{(2 - r_{n-1}^2)^2}.$$

Substituting these relations in g_n , and after some lengthy calculations we obtain

$$(3.33) \quad g_n = \frac{(1 - r_{n-1}^2)^2}{(2 - r_{n-1}^2)^4} (-r_{n-1}^6 + 15r_{n-1}^4 - 64r_{n-1}^2 + 66).$$

Now for $r_{n-1}^2 \in [0, 1)$, we have

$$1 - r_{n-1}^2 > 0, \quad 2 - r_{n-1}^2 > 0, \quad 66 - 64r_{n-1}^2 > 0, \quad 15r_{n-1}^4 - r_{n-1}^6 \geq 0,$$

which proves that $g_n > 0$, and that $a_{n+1}^2 - 36 > 96(1 - r_n^2)$. Therefore, the inequality (3.30) holds for all $\ell = 0, 1, \dots$

To prove the monotonicity of $c_{\ell,C}^2$, we show that

$$(3.34) \quad f_\ell := c_{\ell+1,C}^2 / c_{\ell,C}^2 < 1.$$

Using (3.29) we get

$$f_\ell = \frac{(1 - r_\ell^2)(a_\ell^2 - 36)}{(1 - r_{\ell-1}^2)(a_{\ell+1}^2 - 36)}.$$

Multiplying numerator and denominator by $(2 - r_\ell^2)^2$, we obtain

$$\begin{aligned} f_\ell &= \frac{(1 - r_\ell^2) \left((2 - r_\ell^2)^2 a_\ell^2 - 36(2 - r_\ell^2)^2 \right)}{(1 - r_{\ell-1}^2)(a_{\ell+1}^2 - 36)(2 - r_\ell^2)^2} \\ &= \frac{(1 - r_\ell^2) \left(a_{\ell+1}^2 - 36 + 36(1 - (2 - r_\ell^2)^2) \right)}{(1 - r_{\ell-1}^2) (a_{\ell+1}^2 - 36)(2 - r_\ell^2)^2} \\ &= \frac{(1 - r_\ell^2)}{(1 - r_{\ell-1}^2)(2 - r_\ell^2)^2} + \frac{36(1 - r_\ell^2)(1 - (2 - r_\ell^2)^2)}{(1 - r_{\ell-1}^2)(a_{\ell+1}^2 - 36)(2 - r_\ell^2)^2}. \end{aligned}$$

Now since $c_{\ell+1,C}^2 < 3/8$, we have $(1 - r_\ell^2)/(a_{\ell+1}^2 - 36) < 1/96$ from (3.30). Therefore,

$$\begin{aligned} f_\ell &< \frac{(1 - r_\ell^2)}{(1 - r_{\ell-1}^2)(2 - r_\ell^2)^2} + \frac{36(1 - (2 - r_\ell^2)^2)}{96(1 - r_{\ell-1}^2)(2 - r_\ell^2)^2} \\ &= \frac{(1 - r_\ell^2) + \frac{3}{8}(1 - (2 - r_\ell^2)^2)}{(1 - r_{\ell-1}^2)(2 - r_\ell^2)^2} = \frac{11/8 - r_\ell^2 - \frac{3}{8}(2 - r_\ell^2)^2}{(1 - r_{\ell-1}^2)(2 - r_\ell^2)^2}. \end{aligned}$$

This gives

$$\begin{aligned} f_\ell - 1 &< \frac{11/8 - r_\ell^2 - \frac{3}{8}(2 - r_\ell^2)^2 - (1 - r_{\ell-1}^2)(2 - r_\ell^2)^2}{(1 - r_{\ell-1}^2)(2 - r_\ell^2)^2} \\ &= \frac{11/8 - r_\ell^2 + (2 - r_\ell^2)^2(-11/8 + r_{\ell-1}^2)}{(1 - r_{\ell-1}^2)(2 - r_\ell^2)^2}. \end{aligned}$$

Using (3.32) we therefore get

$$f_\ell - 1 < \frac{-8\ell}{(1 - r_{\ell-1}^2)(2 - r_\ell^2)^2} < 0,$$

since $g_\ell > 0$, $1 - r_{\ell-1}^2 > 0$, and $(2 - r_\ell^2)^2 > 0$. This proves (3.34) and concludes the proof. \square

Lemma 3.4. *Let $e > 0$ and the sequences a_ℓ and b_ℓ be as defined in Lemma 3.2. Then for*

$$(3.35) \quad c_{\ell,D}^2 = \frac{72(a_\ell + b_\ell)}{(a_\ell + 12)(a_\ell - 6)(a_\ell - b_\ell)},$$

the following bounds hold for all $\ell = 0, 1, 2, \dots$

$$(3.36) \quad c_{\ell,D}^2 < c_{\ell-1,D}^2 < \dots < c_{1,D}^2 < c_{0,D}^2 < 1/2.$$

Proof. Substituting the relations for $a_0, b_0, a_0 - b_0, a_0 + b_0, a_0 - 6$, and $a_0 + 6$ from Lemma 3.3 in the definition of $c_{0,D}^2$, we get

$$(3.37) \quad c_{0,D}^2 = \frac{54}{(e + 9)(e + 12)} < 1/2.$$

Now substituting the values of a_0, a_1, b_0 and b_1 , and after some lengthy, but simple calculations, we find that

$$(3.38) \quad c_{1,D}^2 - c_{0,D}^2 = \frac{-486e(5e^2 + 88e + 372)}{(e + 9)(e + 12)(7e + 48)(7e^2 + 84e + 108)} < 0.$$

For remaining bounds, we use induction and proceed as follows. Let $t_m := 1/2 - c_{m,D}^2$ and $t_{m+1} := 1/2 - c_{m+1,D}^2$. Then, expanding a_{m+1} and b_{m+1} in terms of a_m and b_m , and dropping the subscripts of a_m and b_m for brevity reasons, we get

$$(3.39a) \quad t_m := 1/2 - c_{m,D}^2 = \frac{-216a + 6a^2 + a^3 - 72b - 6ab - a^2b}{2(a-6)(a+12)(a-b)} =: \frac{n_m}{d_m},$$

$$(3.39b) \quad t_{m+1} := 1/2 - c_{m+1,D}^2 = \frac{-216a^2 + 12a^3 + 4a^4 + 144b^2 - 6ab^2 - 4a^2b^2 + b^4}{2(-6a + 2a^2 - b^2)(12a + 2a^2 - b^2)} =: \frac{n_{m+1}}{d_{m+1}},$$

where n_m and n_{m+1} are the numerators of t_m and t_{m+1} , respectively, and d_m and d_{m+1} are the denominators of t_m and t_{m+1} , respectively. Assume that the relation (3.36) holds for $\ell = m \geq 1$, i.e., $t_m > 0$. We need to show that $t_{m+1} > 0$. Since $a > 6$, $a > |b|$, and $b < 0$ for $m \geq 1$, we see that d_m and d_{m+1} are positive. Therefore, it suffices to show that n_{m+1} is positive whenever n_m is positive. Given $a/2 > 1$, we consider $n_{m+1} - \frac{a}{2}n_m$. We have

$$\begin{aligned} 2(n_{m+1} - \frac{a}{2}n_m) &= (a+b)(7a^3 + 18a^2 - 6a^2b + 288b + 2b^3 - 216a - 12ab - 2ab^2) \\ &= (a+b)(-6b(a^2 + 2a - 48) + 3a(a^2 + 6a - 72) + 2(a^3 + b^3) + 2a(a^2 - b^2)) \\ &> 0, \end{aligned}$$

since $a > 6$, $a > |b|$, and $b < 0$ for $m \geq 1$. This proves that $n_{m+1} > 0$, and hence, $t_{m+1} > 0$.

The monotonicity of $c_{\ell,D}^2$ can be shown by using (3.38) and showing the induction that $c_{m+1,D}^2 - c_{m,D}^2 < 0$ whenever $c_{m,D}^2 - c_{m-1,D}^2 < 0$. The details are omitted here (the results can also be verified by using algebraic cylindrical decomposition in a computer algebra system like Mathematica [31]). \square

The sequences a_ℓ , b_ℓ , and r_ℓ are plotted in Figure 4, and the sequences $c_{\ell,C}^2$ and $c_{\ell,D}^2$ are plotted in Figure 5.

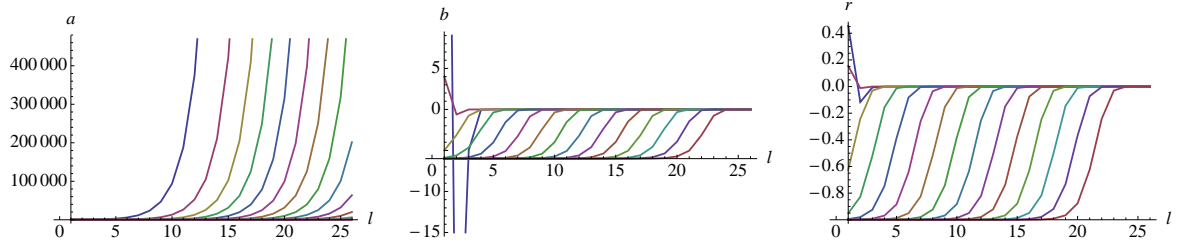


FIGURE 4. a_ℓ , b_ℓ , and r_ℓ for $e = 10^{m_0}$, where $m_0 = \{2, 1, 0, \dots - 11, -12\}$ (left to right)

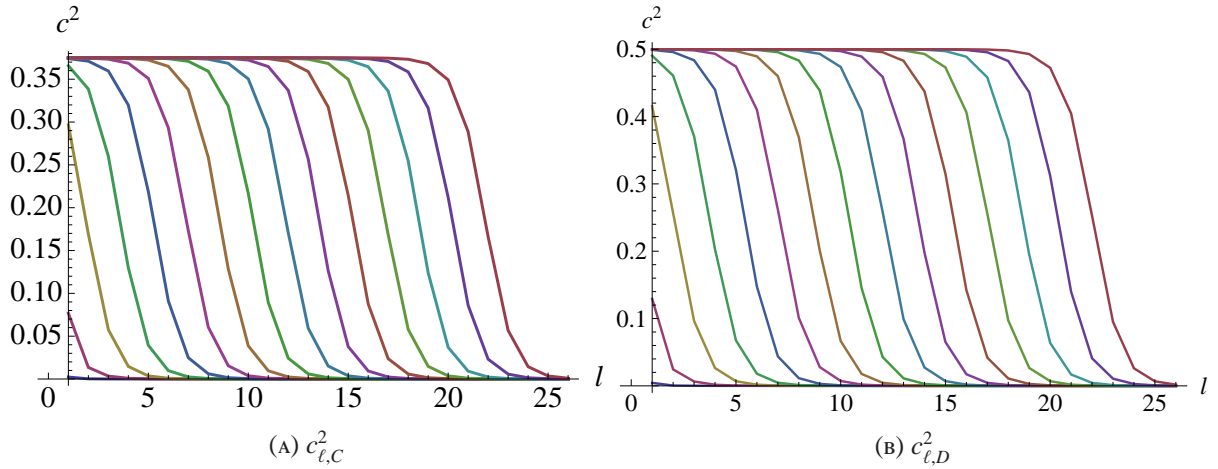


FIGURE 5. c_ℓ^2 for $e = 10^{m_0}$, where $m_0 = \{2, 1, 0, \dots - 11, -12\}$ (left to right)

We are now in a position to prove the following theorem which provides a theoretical estimate that holds on all levels of recursive splitting of the N^0 subspace of $H(\text{curl})$, and RTN^0 subspace of $H(\text{div})$.

Theorem 3.5. Consider the bilinear form (1.1), where $0 < \alpha, \beta < \infty$, and the related discrete problem (1.5) on the N^0 subspace of two-dimensional $H(\text{curl})$ or RTN^0 subspace of three-dimensional $H(\text{div})$. Assuming that the underlying mesh is uniform, the CBS constant γ related to the hierarchical splitting (3.19) has the upper bound $\gamma \leq \gamma_G < \sqrt{\Theta}$, where Θ is $3/8$ for two-dimensional $H(\text{curl})$ problem, and $1/2$ for three-dimensional $H(\text{div})$ problem. This upper bound holds for each step of the recursive hierarchical splitting. Moreover, $\gamma^{(L-\ell)}$ is monotonically strictly decreasing and has an upper bound of $\sqrt{\Theta}$ for all $\ell = 0, 1, \dots, L$, i.e.,

$$(3.40) \quad \gamma^{(0)} < \gamma^{(1)} < \dots < \gamma^{(\ell)} < \dots < \gamma^{(L-1)} < \gamma^{(L)} < \sqrt{\Theta}.$$

Proof. In order to prove this uniform bound for γ we study the generalized eigenproblem (3.20). At level L of the finest discretization the macro-element matrix \hat{A}_G , which is the same for all G in \mathcal{T}_{h_L} for a uniform mesh, can be represented in the form

$$(3.41) \quad \hat{A}_G^{(L)} = J_G \left(\sum_{K \in G \subset \mathcal{T}_{h_\ell}} R_K^T A_K^{(L)} R_K \right) J_G^T.$$

We first focus on two-dimensional $H(\text{curl})$ problem, for which

$$(3.42) \quad A_{K,C}^{(L)} = \frac{\beta}{6h^2} \begin{bmatrix} a_0 & b_0 & -6 & 6 \\ b_0 & a_0 & 6 & -6 \\ -6 & 6 & a_0 & b_0 \\ 6 & -6 & b_0 & a_0 \end{bmatrix}, \quad \forall K \in G, \forall G \subset \mathcal{T}_{h_L}.$$

The variables a_0 and b_0 are defined in Lemma 3.2, e and κ are defined before (2.6), and the local transformation matrix J_G is defined according to (3.13). The lower-right 4×4 block of the matrix B_G and the Schur complement S_G for the first splitting (at level L) are to be found

$$(3.43a) \quad B_{G,22}^{(L)} = \frac{\beta}{6h^2} \begin{bmatrix} p_0 & q_0 & -3/2 & 3/2 \\ q_0 & p_0 & 3/2 & -3/2 \\ -3/2 & 3/2 & p_0 & q_0 \\ 3/2 & -3/2 & q_0 & p_0 \end{bmatrix},$$

$$(3.43b) \quad S_G^{(L)} = \frac{\beta}{6h^2} \begin{bmatrix} s_0 & t_0 & -3/2 & 3/2 \\ t_0 & s_0 & 3/2 & -3/2 \\ -3/2 & 3/2 & s_0 & t_0 \\ 3/2 & -3/2 & t_0 & s_0 \end{bmatrix}.$$

with

$$\begin{aligned} q_0 &= -b_0^2/4a_0, & p_0 &= a_0/2 + q_0, \\ t_0 &= \frac{36a_0 + 72b_0 + a_0b_0^2}{144 - 4a_0^2}, & s_0 &= a_0/2 + t_0. \end{aligned}$$

The generalized eigenproblem (3.20) has two different two-fold eigenvalues, namely $\lambda_{1,2} = 1$ and

$$\lambda_{3,4} = \frac{a_0(a_0^2 - a_0b_0 - 72)}{(a_0^2 - 36)(a_0 - b_0)},$$

which shows that

$$(3.44) \quad \left(\gamma_G^{(L)} \right)^2 \leq 1 - \lambda_{3,4} = \frac{36(a_0 + b_0)}{(a_0^2 - 36)(a_0 - b_0)}.$$

Note that the coefficient β does not appear in the bound for γ since the factor $\frac{\beta}{6h^2}$ appear in both the matrices of the generalized eigenproblem (3.20), and thus does not affect the eigenvalues.

Now in order to compute a similar bound for the second splitting (at level $L-1$) we have to use the relation $A_K^{(L-1)} := B_{G,22}^{(L)}$. In general, for the $(\ell+1)$ th splitting (at level $L-\ell$) the relation

$$(3.45) \quad A_K^{(L-\ell)} := B_{G,22}^{(L-\ell+1)}$$

is to be used in the assembly of $\hat{A}_G^{L-\ell}$, i.e.,

$$(3.46) \quad \hat{A}_G^{(L-\ell)} = J_G \left(\sum_{K \in G \subset \mathcal{T}_{h_{L-\ell}}} R_K^T A_K^{(L-\ell)} R_K \right) J_G^T.$$

Repeating the computations, we find that the relation (3.46) holds for all levels $\ell = 1, 2, \dots, L-1, L$, and the element stiffness matrix $A_K^{L-\ell}$ (after ℓ coarsening steps) is given by

$$(3.47) \quad A_{K,C}^{(L-\ell)} = \frac{\beta}{6(2^\ell h)^2} \begin{bmatrix} a_\ell & b_\ell & -6 & 6 \\ b_\ell & a_\ell & 6 & -6 \\ -6 & 6 & a_\ell & b_\ell \\ 6 & -6 & b_\ell & a_\ell \end{bmatrix}, \quad \forall K \in G, \forall G \subset \mathcal{T}_{h_{L-\ell}},$$

where the sequences a_ℓ and b_ℓ are defined in (3.22). Thus, the bound for γ_G at level $L - \ell$ reads

$$(3.48) \quad (\gamma_G^{(L-\ell)})^2 = \frac{36(a_\ell + b_\ell)}{(a_\ell^2 - 36)(a_\ell - b_\ell)}.$$

The result (3.40) then follows by taking $\gamma_G^{L-\ell} = c_{\ell,C}$, where $c_{\ell,C}$ is defined in Lemma 3.3.

For three-dimensional $H(\text{div})$ problem we have

$$(3.49) \quad A_{K,D}^{(L)} = \frac{\beta}{6h^3} \begin{bmatrix} a_0 & b_0 & 6 & -6 & 6 & -6 \\ b_0 & a_0 & -6 & 6 & -6 & 6 \\ 6 & -6 & a_0 & b_0 & 6 & -6 \\ -6 & 6 & b_0 & a_0 & -6 & 6 \\ 6 & -6 & 6 & -6 & a_0 & b_0 \\ -6 & 6 & -6 & 6 & b_0 & a_0 \end{bmatrix}, \quad \forall K \in G, \forall G \subset \mathcal{T}_{h_L},$$

and the local transformation matrix J_G is defined according to (3.14). The lower-right 6×6 block of the matrix B_G and the Schur complement S_G for the first splitting (at level L) are to be found (using e.g., Mathematica [31])

$$(3.50a) \quad B_{G,22}^{(L)} = \frac{\beta}{6h^3} \begin{bmatrix} p_0 & q_0 & 3/4 & -3/4 & 3/4 & -3/4 \\ q_0 & p_0 & -3/4 & 3/4 & -3/4 & 3/4 \\ 3/4 & -3/4 & p_0 & q_0 & 3/4 & -3/4 \\ -3/4 & 3/4 & q_0 & p_0 & -3/4 & 3/4 \\ 3/4 & -3/4 & 3/4 & -3/4 & p_0 & q_0 \\ -3/4 & 3/4 & -3/4 & 3/4 & q_0 & p_0 \end{bmatrix},$$

$$(3.50b) \quad S_G^{(L)} = \frac{\beta}{6h^3} \begin{bmatrix} s_0 & t_0 & 3/4 & -3/4 & 3/4 & -3/4 \\ t_0 & s_0 & -3/4 & 3/4 & -3/4 & 3/4 \\ 3/4 & -3/4 & s_0 & t_0 & 3/4 & -3/4 \\ -3/4 & 3/4 & t_0 & s_0 & -3/4 & 3/4 \\ 3/4 & -3/4 & 3/4 & -3/4 & s_0 & t_0 \\ -3/4 & 3/4 & -3/4 & 3/4 & t_0 & s_0 \end{bmatrix},$$

with

$$\begin{aligned} q_0 &= -b_0^2/8a_0, & p_0 &= a_0/4 + q_0, \\ t_0 &= \frac{-72a_0 - 144b_0 - 6b_0^2 - a_0b_0^2}{8(a_0 - 6)(a_0 + 12)}, & s_0 &= a_0/4 + t_0. \end{aligned}$$

The generalized eigenproblem (3.20) has two different three-fold eigenvalues, namely $\lambda_{1,2,3} = 1$ and

$$\lambda_{4,5,6} = \frac{a_0(a_0^2 - a_0b_0 + 6a_0 - 6b_0 - 144)}{(a_0 + 12)(a_0 - 6)(a_0 - b_0)},$$

which shows that

$$(3.51) \quad (\gamma_G^{(L)})^2 \leq 1 - \lambda_{4,5,6} = \frac{72(a_0 + b_0)}{(a_0 + 12)(a_0 - 6)(a_0 - b_0)}.$$

As before, to compute a similar bound for the $(\ell + 1)^{\text{th}}$ splitting the relation (3.45) is to be used in the assembly of $\hat{A}_G^{L-\ell}$, see (3.46). Repeating the computations, we find that the relation (3.46) holds for all levels $\ell = 1, 2, \dots, L - 1, L$, and the element stiffness matrix $A_K^{L-\ell}$ (after ℓ coarsening steps) is given by

$$(3.52) \quad A_{K,D}^{(L-\ell)} = \frac{\beta}{6(2^\ell h)^3} \begin{bmatrix} a_\ell & b_\ell & 6 & -6 & 6 & -6 \\ b_\ell & a_\ell & -6 & 6 & -6 & 6 \\ 6 & -6 & a_\ell & b_\ell & 6 & -6 \\ -6 & 6 & b_\ell & a_\ell & -6 & 6 \\ 6 & -6 & 6 & -6 & a_\ell & b_\ell \\ -6 & 6 & -6 & 6 & b_\ell & a_\ell \end{bmatrix}, \quad \forall K \in G, \forall G \subset \mathcal{T}_{h_{L-\ell}}.$$

Thus, the bound for γ_G at level $L - \ell$ reads

$$(3.53) \quad (\gamma_G^{(L-\ell)})^2 = \frac{72(a_\ell + b_\ell)}{(a_\ell + 12)(a_\ell - 6)(a_\ell - b_\ell)}.$$

The result (3.40) then follows by taking $\gamma_G^{L-\ell} = c_{\ell,D}$, where $c_{\ell,D}$ is defined in Lemma 3.4. \square

Remark 3.6. The curves in Figure 5 show the behavior of γ_G^2 (defined by (3.48) and (3.53)). We observe that γ_G^2 approaches zero when the splitting is applied many times (increasing ℓ from left to right), which means that the two subspaces \mathcal{V}_1 and \mathcal{V}_2 in (3.19) become increasingly orthogonal to each other as the recursion proceeds. Therefore, on (very) coarse levels, the upper bound Θ for γ_G^2 , and thus for γ^2 , is quite pessimistic.

Remark 3.7. Note that the lowest order Raviart-Thomas (respectively Raviart-Thomas-Nedelec) type elements on general quadrilateral (respectively hexahedral) meshes do not show any convergence for the divergence of the field [1]. In such cases, one can use, e.g., Arnold-Boffi-Falk type elements [1]. However, the presented analysis won't suffice for such elements, and further work will be needed.

4. ALGORITHMIC ASPECTS

In this section we present the algorithms which have been used in this article for the solution of $Mz = r$, the step used in preconditioned conjugate gradient method (PCG) for linear AMLI or flexible conjugate gradient method (FCG) for nonlinear AMLI. The algorithms, presented as pseudocodes with a compact syntax/style close to the `matlab`[®] language [32], should be helpful to the practitioners in the respective fields*. The preconditioner M , as explained in Section 3.1, requires the solution of nested systems $\hat{A}z = r$, and $Bv = w$, where the matrices \hat{A} and B are defined in (3.17) and (3.18), respectively. Using the factorization (3.17) we rewrite $\hat{A}z = r$ as follows

$$(4.1) \quad \begin{bmatrix} \hat{A}_{11} & 0 \\ \hat{A}_{21} & B \end{bmatrix} \begin{bmatrix} y_1 \\ y_2 \end{bmatrix} = \begin{bmatrix} r_1 \\ r_2 \end{bmatrix}, \quad \begin{bmatrix} I_1 & \hat{A}_{11}^{-1}\hat{A}_{12} \\ 0 & I_2 \end{bmatrix} \begin{bmatrix} z_1 \\ z_2 \end{bmatrix} = \begin{bmatrix} y_1 \\ y_2 \end{bmatrix}.$$

Similarly, using the partitioning (3.18) we rewrite $Bv = w$ as follows

$$(4.2) \quad \begin{bmatrix} B_{11} & 0 \\ B_{21} & B_{22} \end{bmatrix} \begin{bmatrix} t_1 \\ t_2 \end{bmatrix} = \begin{bmatrix} w_1 \\ w_2 \end{bmatrix}, \quad \begin{bmatrix} I_3 & B_{11}^{-1}B_{12} \\ 0 & I_4 \end{bmatrix} \begin{bmatrix} v_1 \\ v_2 \end{bmatrix} = \begin{bmatrix} t_1 \\ t_2 \end{bmatrix}.$$

Note that in (4.2) the matrix B_{22} is an approximation of the exact Schur complement $S = B_{22} - B_{21}B_{11}^{-1}B_{12}$. Given the *exact* LU factors $L_{11}^{\hat{A}}$ and $U_{11}^{\hat{A}}$ of \hat{A}_{11} , and incomplete LU factors L_{11}^B and U_{11}^B of B_{11} , the Algorithms 1 and 2 solve the triangular systems in (4.1)-(4.2). Note that, since $v_2 = t_2$, the solution of

$$B_{22}v_2 = w_2 - B_{21}t_1 =: w_c$$

is performed at the next coarser level with the recursive application of AMLI algorithm.

We now first present the algorithm for the linear AMLI method. This algorithm is adapted from [8, 25, 42]. The linear AMLI algorithm requires the computation of coefficients $q_i, i = 0 \dots \nu - 1$, from properly shifted and scaled Chebyshev polynomials. The algorithm presented below is for fixed V - or ν -cycle for all levels (ν -cycle also has the V -cycle at the finest level), which is commonly used in practice. For varying V - or ν -cycles at any given level (and thus having more involved algorithm), see e.g., [25, Alg. 10.1].[†]

*The variable names listed in **Require** may be defined globally or passed as arguments.

[†]The vector $d^{(k-1)}$ in the right hand side of [25, (10.6)] is erroneous, and should be replaced by $w^{(k-1)}$, see [8, (3.6)].

Algorithm 1 Solve lower triangular system**Require:** $L_{11}^A, U_{11}^A, \hat{A}_{12}, L_{11}^B, U_{11}^B, B_{12}$ **function** $[y_1, t_1, w_c] = \text{SOLVEL}(r)$

$$y_1 = U_{11}^A \setminus (L_{11}^A \setminus r_1); \quad w = r_2 - (\hat{A}_{12})^T y_1;$$

▷ See (4.1) for the dimensions of r_1 and r_2

$$t_1 = U_{11}^B \setminus (L_{11}^B \setminus w_1);$$

▷ See (4.2) for the dimensions of w_1 and w_2 **if** preconditioner is additive **then**

$$w_c = w_2;$$

else

$$w_c = w_2 - (B_{12})^T t_1;$$

end if**end function****Algorithm 2** Solve upper triangular system**Require:** $L_{11}^A, U_{11}^A, \hat{A}_{12}, L_{11}^B, U_{11}^B, B_{12}$ **function** $z = \text{SOLVEU}(v_2, t_1, y_1)$ **if** preconditioner is additive **then**

$$v_1 = t_1;$$

else

$$v_1 = t_1 - U_{11}^B \setminus (L_{11}^B \setminus (B_{12} v_2));$$

end if

$$z_2 = [v_1; v_2]; \quad z_1 = y_1 - U_{11}^A \setminus (L_{11}^A \setminus (\hat{A}_{12} z_2)); \quad z = [z_1; z_2];$$

end function**Algorithm 3** Linear AMLI**Require:** v, q, J, B_{22} **function** $z = \text{LAMLI}(r, L, \ell)$

$$r = Jr; \quad [y_1, t_1, w_c] = \text{SOLVEL}(r);$$

if $\ell = L$ **then**

▷ Finest level, only V-cycle

$$r_c = w_c; \quad v_2 = \text{SOLVEV2}(r_c, L, \ell);$$

else▷ Coarser levels, V- or ν -cycle

$$r_c = q_{v-1} w_c; \quad v_2 = \text{SOLVEV2}(r_c, L, \ell);$$

for $\sigma = 2 : v$ **do**

$$r_c = B_{22} v_2 + q_{v-\sigma} w_c; \quad v_2 = \text{SOLVEV2}(r_c, L, \ell);$$

end for**end if**

$$z = \text{SOLVEU}(v_2, t_1, y_1); \quad z = J^T z;$$

end function**function** $v_2 = \text{SOLVEV2}(r_c, L, \ell)$ **if** $\ell - 1 = 0$ **then**

$$v_2 = B_{22} \setminus r_c;$$

▷ Exact solve at coarsest level

else

$$v_2 = \text{LAMLI}(r_c, L, \ell - 1);$$

▷ Recursive call to LAMLI for intermediate levels

end if**end function**

Finally, we present the nonlinear AMLI algorithm. This algorithm is adapted from [8, 10, 25, 34, 35, 42]. Again, the algorithm presented below is for fixed V- or ν -cycle for all levels, and thus has simpler presentation than for varying V- or ν -cycles at any given level (see e.g., [25, Alg. 10.2], [10, Alg. 5.4] or [35, Alg. 6.1] for the latter). ‡

‡The algorithm presented in [25, Alg. 10.2] recursively updates the vector q in the **for** loop on j , which is not what was originally proposed in other two references.

Algorithm 4 Nonlinear AMLI**Require:** ν, J, \hat{A}, B_{22} **function** $z = \text{NAMLI}(r, L, \ell)$ $z = 0$; $r = Jr$; $[y_1, t_1, r_c] = \text{SOLVE}(r)$; $v_2 = \text{SOLVEV2}(r_c, L, \ell)$;**if** $\ell = L$ **then** \triangleright Finest level, only V-cycle $p = \text{SOLVEU}(v_2, t_1, y_1)$; $z = z + p$;**else** \triangleright Coarser levels, V- or ν -cycle $p_1 = \text{SOLVEU}(v_2, t_1, y_1)$; $q_1 = \hat{A}p_1$; $\tau_1 = p_1^T q_1$; $\alpha = (r^T, p_1)/\tau_1$; $z = z + \alpha p_1$; $r = r - \alpha q_1$;**for** $\sigma = 2 : \nu$ **do** $[y_1, t_1, r_c] = \text{SOLVE}(r)$; $v_2 = \text{SOLVEV2}(r_c, L, \ell)$; $p_\sigma = \text{SOLVEU}(v_2, t_1, y_1)$; $s = 0$;**for** $j = 1 : \sigma - 1$ **do** $\beta = (p_\sigma^T q_j)/\tau_j$; $s = s - \beta p_j$;**end for** $p_\sigma = p_\sigma + s$; $q_\sigma = \hat{A}p_\sigma$; $\tau_\sigma = p_\sigma^T q_\sigma$; $\alpha = (r^T p_\sigma)/\tau_\sigma$; $z = z + \alpha p_\sigma$; $r = r - \alpha q_\sigma$;**end for****end if** $z = J^T z$;**end function****function** $v_2 = \text{SOLVEV2}(r_c, L, \ell)$ **if** $\ell - 1 = 0$ **then** $v_2 = B_{22} \setminus r_c$; \triangleright Exact solve at coarsest level**else** $v_2 = \text{NAMLI}(r_c, L, \ell - 1)$; \triangleright Recursive call to NAMLI for intermediate levels**end if****end function**

5. NUMERICAL RESULTS

All the numerical experiments presented in this section are performed using `matlab`[®] R2012b on an HP Z420 workstation with 12 core 3.2 GHz CPU and 64 GB RAM. The initial guess is chosen as a zero vector, and the stopping criteria is chosen as $\epsilon \leq 10^{-8}$, where ϵ and the average residual reduction factor ρ are defined as

$$\epsilon := \|r^{(n_{\text{it}})}\| / \|r^{(0)}\|, \quad \rho := \epsilon^{\frac{1}{n_{\text{it}}}},$$

and n_{it} is the number of iterations reported in the tables.

5.1. Two-dimensional $H(\text{curl})$ problem. We first present numerical results for two-dimensional $H(\text{curl})$ problem. For all the numerical experiments, we consider a mesh of square elements of size $h = 1/8, 1/64, \dots, 1/2048$ (i.e., up to 8,392,704 DOF for the finest level). We use a direct solver on the coarsest mesh that consists of 4×4 elements. Hence, the multilevel procedure is based on 1 to 9 levels of regular mesh refinement (resulting in an ℓ -level method, $\ell = 3, \dots, 11$).

Example 5.1. Consider the model problem (1.1) in a unit square, and fix the coefficients $\alpha = \beta = 1$. The problem data is chosen such that the exact solution is given by $\mathbf{u} = (\pi \sin \pi x \cos \pi y, -\pi \cos \pi x \sin \pi y)^T$.

For the W -cycle method, we chose two-types of stabilization polynomials $q^{(\ell)}$. One is based on Chebyshev polynomials (see, e.g., [8, 25, 42], denoted in the tables by T), for which the polynomial $q^{(\ell)}(x)$ is defined as $2/(s-b) - x/(s-b)^2$, where $s = \sqrt{1+b+b^2-\gamma^2}$, and b is some constant estimating the upper bound of the condition number of preconditioned B_{11} block, see the Appendix for details. The other one is based on the polynomial of best uniform approximation to $1/x$ (see, e.g., [29], denoted in the tables by X), for which the polynomial $q^{(\ell)}(x)$ is defined as $(2-\gamma^2)/(1-\gamma^2) - x/(1-\gamma^2)$. The

results for the V -cycle and W -cycle multiplicative AMLI method are presented in Table 1. The second column confirms the error convergence behavior. We see that for decreasing h the growth in the iteration number for V -cycle is moderate (as expected), whereas both the W -cycle versions (T and X) exhibit h -independence. Moreover, the total time (factorization and solver) reported in eighth and eleventh columns also confirms that both the versions of W -cycle are of practical optimal complexity (slight increase in time may be attributed to the implementation issues). We note that in the multiplicative preconditioning the X -version W -cycle gives slightly better results than the T -version W -cycle.

TABLE 1. Convergence results for multiplicative AMLI, $\alpha = \beta = 1, \chi = \mathbf{u} - \mathbf{u}_h$

$1/h$	$\ \text{curl}\chi\ _{L^2(\Omega)}$	V -cycle			W -cycle (T)			W -cycle (X)		
		n_{it}	ρ	t_{sec}	n_{it}	ρ	t_{sec}	n_{it}	ρ	t_{sec}
8	0.15946423	7	0.049	0.00	7	0.049	0.00	7	0.049	0.00
16	0.08005229	8	0.094	0.01	8	0.083	0.01	8	0.094	0.01
32	0.04006629	10	0.143	0.01	9	0.104	0.01	8	0.097	0.01
64	0.02003817	11	0.174	0.04	9	0.105	0.05	8	0.100	0.04
128	0.01001971	12	0.201	0.14	9	0.108	0.16	8	0.095	0.14
256	0.00500993	13	0.224	0.54	9	0.109	0.55	8	0.088	0.51
512	0.00250498	14	0.246	2.41	9	0.110	2.22	8	0.083	2.09
1024	0.00125249	14	0.267	10.74	9	0.110	9.35	8	0.078	8.99
2048	0.00062624	16	0.313	49.79	9	0.110	40.29	8	0.073	38.74

We now test the AMLI method with additive preconditioning. The results for the V -cycle and both the W -cycle additive AMLI methods are presented in Table 2. We also present the results for nonlinear variant of AMLI method, see e.g., [9, 10, 24, 25, 34, 35, 36], in the last three columns (denoted in the tables by N , W -cycle referring to two inner iterations). Surprisingly, in the additive form, the T -version W -cycle gives much better results than the X -version W -cycle, where the latter appears to be stabilizing only towards very fine mesh (many recursive levels). This can be attributed to the fact that for the additive preconditioning, for the choice of $\gamma = \sqrt{3/8}$, we require that $\nu > \sqrt{(1+\gamma)/(1-\gamma)} > 2$, which does not hold for (both) the W -cycle. The results of nonlinear W -cycle further improve the results of T -version W -cycle (linear). Since the nonlinear W -cycle AMLI method gives the best results (and is free from parameters b and γ), in the remaining numerical experiments we will only present the results from multiplicative form of V -cycle and nonlinear W -cycle AMLI method.

TABLE 2. Convergence results for additive AMLI, $\alpha = \beta = 1$

$1/h$	V -cycle			W -cycle (T)			W -cycle (X)			W -cycle (N)		
	n_{it}	ρ	t_{sec}	n_{it}	ρ	t_{sec}	n_{it}	ρ	t_{sec}	n_{it}	ρ	t_{sec}
8	10	0.153	0.00	10	0.153	0.00	10	0.153	0.00	10	0.153	0.00
16	17	0.300	0.01	17	0.299	0.01	17	0.299	0.01	12	0.208	0.01
32	20	0.391	0.02	19	0.346	0.03	23	0.446	0.03	12	0.209	0.03
64	25	0.472	0.06	19	0.372	0.08	31	0.550	0.13	12	0.197	0.08
128	30	0.538	0.21	21	0.386	0.26	44	0.653	0.47	11	0.179	0.23
256	34	0.575	0.87	19	0.377	0.79	56	0.712	1.82	11	0.167	0.76
512	39	0.617	3.99	19	0.361	3.04	60	0.735	6.85	9	0.127	2.61
1024	44	0.657	19.20	19	0.362	12.46	65	0.751	28.90	9	0.117	10.65
2048	50	0.685	91.72	19	0.371	52.99	65	0.752	121.49	8	0.098	43.03

Example 5.2. Consider the model problem (1.1) in a unit square, fix the coefficient $\beta = 1$ and take $\alpha = 10^{m_0}$ for $m_0 = \{-6, -3, 0, 3, 6\}$. The right hand side (RHS) vector is all ones.

The results for the multiplicative AMLI method for varying α are presented in Table 3 for V - and nonlinear W -cycle. We see that the V -cycle shows some effect of α , with a moderate growth in the number of iterations for decreasing h , however, the nonlinear W -cycle is independent of h , and is fully robust with respect to α . Note that towards very large values of α , the system matrix is well-conditioned,

and the hierarchical splitting approaches orthogonal decomposition, therefore, the V -cycle method also exhibits optimal order complexity.

TABLE 3. Convergence results for multiplicative AMLI, $\beta = 1, \alpha = 10^{m_0}$

$\alpha \rightarrow$	n_{it}									
	10^{-6}		10^{-3}		10^0		10^3		10^6	
$1/h$	V	W	V	W	V	W	V	W	V	W
8	9	9	9	9	9	9	4	4	2	2
16	12	10	12	10	12	10	7	6	2	2
32	15	10	15	10	14	10	9	8	2	2
64	17	10	17	10	16	10	11	9	2	2
128	20	9	20	9	17	9	12	9	3	3
256	22	9	22	9	18	9	14	9	4	4
512	26	9	26	9	21	9	16	9	6	6
1024	28	9	28	9	23	9	17	9	8	8
2048	28	9	31	8	25	8	20	8	10	8

Example 5.3. Consider the model problem (1.1) in a unit square, fix the coefficient $\alpha = 1$ and take $\beta = 10^{m_0}$ for $m_0 = \{-6, -3, 0, 3, 6\}$. The RHS vector is all ones.

The results for the multiplicative AMLI method for varying β are presented in Table 4 for V - and W -cycles. The results are qualitatively the same as in Table 3 for varying α , with the parameter value reversing the behavior of the solver.

Example 5.4. Consider the model problem (1.1) in a unit square, and fix the coefficient $\beta = 1$. The coefficient α is chosen as 1 in $[0, 0.5]^2 \cup (0.5, 1]^2$ and κ elsewhere, where $\kappa = 10^{m_0}$, and $m_0 = \{-6, -4, -2, 0\}$. The RHS vector is all ones.

Finally, the results for the multiplicative AMLI method for the case with jump in the coefficients (aligned with the coarsest level mesh), which are presented in Table 5 for V - and nonlinear W -cycles, show robustness with respect to the jump in the coefficients.

5.2. Three-dimensional $H(\text{div})$ problem. We now present the numerical results for three-dimensional $H(\text{div})$ problem. For all the numerical experiments, we consider a uniformly refined mesh of cubic elements of size $h = 1/4, \dots, 1/128$ (i.e., up to 6,340,608 DOF for the finest level). We use a direct solver on the coarsest mesh that consists of 2×2 elements. Hence, the multilevel procedure is based on 1 to 6 levels of regular mesh refinement (resulting in an ℓ -level method, $\ell = 2, \dots, 7$).

Example 5.5. Consider the model problem (1.1) in a unit cube, and fix the coefficients $\alpha = \beta = 1$. The problem data is chosen such that the exact solution is given by $\mathbf{u} = \nabla(\sin \pi x \sin \pi y \sin \pi z)$.

TABLE 4. Convergence results for multiplicative AMLI, $\alpha = 1$

$\beta \rightarrow$	n_{it}									
	10^{-6}		10^{-3}		10^0		10^3		10^6	
$1/h$	V	W	V	W	V	W	V	W	V	W
8	2	2	4	4	9	9	9	9	9	9
16	2	2	7	6	12	10	12	10	12	10
32	2	2	9	8	14	10	15	10	15	10
64	2	2	11	9	16	10	17	10	17	10
128	3	3	12	9	17	9	20	9	20	9
256	4	4	14	9	18	9	22	9	22	9
512	6	6	16	9	21	9	26	9	26	9
1024	8	8	17	9	23	9	28	9	28	9
2048	10	8	20	8	25	8	31	8	28	9

TABLE 5. Convergence results for multiplicative AMLI with jump in the coefficients, $\beta = 1$

$\kappa \rightarrow$	n_{it}							
	10^0		10^{-2}		10^{-4}		10^{-6}	
$1/h$	V	W	V	W	V	W	V	W
8	9	9	10	10	10	10	10	10
16	12	10	12	11	13	11	13	11
32	14	10	15	11	15	11	16	11
64	16	10	17	11	18	11	19	11
128	17	9	20	11	20	11	21	11
256	18	9	22	10	22	11	24	11
512	21	9	23	10	26	11	26	11
1024	23	9	26	10	28	11	28	11
2048	25	8	28	10	32	11	32	11

For the linear AMLI W -cycle, here we only use the stabilization polynomial $q^{(\ell)}(x)$ based on Chebyshev polynomials (and thus omit the notation T). The results for the V -cycle and W -cycle multiplicative AMLI method are presented in Table 6. The second column confirms the error convergence behavior. We see that for decreasing h the growth in the iteration number for V -cycle is moderate (as expected), whereas both the W -cycle versions (linear and nonlinear) exhibit h -independence. Moreover, the total time (setup and solver) reported in eighth and eleventh columns also confirms that both the versions of W -cycle are of practical optimal complexity (slight increase in time may be attributed to the implementation issues). We note that the nonlinear W -cycle gives better results than the linear W -cycle. As a comparison, in the last column we report the timings required for the direct solver in `matlab`[®], which exhibit $O(N_L^2)$ complexity against the optimal $O(N_L)$ complexity of the presented AMLI method.

TABLE 6. Convergence results for multiplicative AMLI, $\alpha = \beta = 1$, $\chi = \mathbf{u} - \mathbf{u}_h$

$1/h$	$\ \text{div}\chi\ _{L^2(\Omega)}$	V-cycle			Linear W-cycle			Nonlinear W-cycle			$A_h \setminus f_h$
		n_{it}	ρ	t_{sec}	n_{it}	ρ	t_{sec}	n_{it}	ρ	t_{sec}	t_{sec}
4	0.37955365	8	0.0992	< 0.01	8	0.0992	< 0.01	8	0.0992	< 0.01	< 0.01
8	0.19467752	10	0.1469	0.02	10	0.1464	0.02	9	0.1020	0.03	0.01
16	0.09796486	12	0.2092	0.11	11	0.1869	0.10	9	0.1147	0.11	0.04
32	0.04906112	14	0.2525	0.81	12	0.1995	0.79	8	0.0958	0.74	1.09
64	0.02454041	15	0.2912	7.10	12	0.1925	6.65	7	0.0684	6.03	63.58
128	0.01227144	17	0.3374	63.04	12	0.2004	56.12	7	0.0608	50.87	5082.70

We now test the AMLI method with additive preconditioning. The results for the V -cycle and both the W -cycle additive AMLI methods are presented in Table 7. Note that for the additive preconditioning, for the choice of $\gamma = \sqrt{1/2}$, we require that $\nu > \sqrt{(1+\gamma)/(1-\gamma)} = 1 + \sqrt{2} > 2$. However, both the W -cycle methods (for $\nu = 2$) exhibit optimal order. This may be attributed to the special structure (and clustering of eigenvalues) of the problem. The results of nonlinear W -cycle further improves the results of linear W -cycle (as compared to the multiplicative version). Since the nonlinear W -cycle AMLI method gives the best results (and is free from parameters b and γ), in the remaining numerical experiments we will only present the results from multiplicative form of V -cycle and nonlinear W -cycle AMLI method.

Example 5.6. Consider the model problem (1.1) in a unit cube, fix the coefficient $\beta = 1$ and take $\alpha = 10^{m_0}$ for $m_0 = \{-6, -3, 0, 3, 6\}$. The right hand side (RHS) vector is all ones.

The results for the multiplicative AMLI method for varying α are presented in Table 8 for V - and nonlinear W -cycle. We see that the V -cycle shows some effect of α , with a moderate growth in the number of iterations for decreasing h , however, the nonlinear W -cycle is independent of h , and is fully robust with respect to α . Note that towards very large values of α , the system matrix is well-conditioned, and the hierarchical splitting approaches orthogonal decomposition, therefore, the V -cycle method also exhibits optimal order complexity. Since fixing α and varying β only reverses the behavior (from left to right) as presented in Table 8, see also Section 5.1, we do not include those results here.

TABLE 7. Convergence results for additive AMLI, $\alpha = \beta = 1$

$1/h$	V-cycle			Linear W-cycle			Nonlinear W-cycle		
	n_{it}	ρ	t_{sec}	n_{it}	ρ	t_{sec}	n_{it}	ρ	t_{sec}
4	12	0.2050	< 0.01	12	0.2050	< 0.01	12	0.2050	< 0.01
8	18	0.3592	0.02	20	0.3736	0.03	15	0.2883	0.03
16	24	0.4640	0.12	28	0.5079	0.15	16	0.2951	0.13
32	30	0.5380	1.03	27	0.5024	1.03	15	0.2840	0.86
64	36	0.5948	9.53	28	0.5077	8.56	14	0.2578	6.91
128	41	0.6329	85.38	28	0.5160	71.13	13	0.2347	56.61

TABLE 8. Convergence results for multiplicative AMLI, $\beta = 1, \alpha = 10^{m_0}$

$\alpha \rightarrow$	n_{it}									
	10^{-6}		10^{-3}		10^0		10^3		10^6	
$1/h$	V	W	V	W	V	W	V	W	V	W
4	12	12	12	12	11	11	3	3	1	1
8	15	13	15	12	15	12	5	5	2	2
16	18	13	18	13	18	13	8	8	2	2
32	21	12	21	12	20	12	11	10	2	2
64	23	12	24	12	24	12	14	11	2	2
128	27	12	25	12	25	12	16	11	3	3

Example 5.7. Consider the model problem (1.1) in a unit cube, and fix the coefficient $\beta = 1$. The coefficient α is chosen as 1 in $[0, 0.5]^3 \cup (0.5, 1]^2 \times [0, 0.5] \cup [0, 0.5] \times (0.5, 1]^2 \cup (0.5, 1] \times [0, 0.5] \times (0.5, 1]$ and κ elsewhere, where $\kappa = 10^{m_0}$, and $m_0 = \{-6, -4, -2, 0\}$. The RHS vector is all ones.

Finally, the results for the multiplicative AMLI method for the case with jump in the coefficients (aligned with the coarsest level mesh), which are presented in Table 9 for V- and nonlinear W-cycles, also show robustness with respect to jumps in the coefficients.

TABLE 9. Convergence results for multiplicative AMLI with jump in the coefficients, $\beta = 1$

$\kappa \rightarrow$	n_{it}							
	10^{-6}		10^{-4}		10^{-2}		10^0	
$1/h$	V	W	V	W	V	W	V	W
4	13	13	13	13	12	12	11	11
8	18	15	17	14	16	13	15	12
16	23	13	20	13	19	13	18	13
32	26	13	24	13	22	13	20	12
64	29	13	27	13	25	13	24	12
128	33	13	30	13	28	13	25	12

6. CONCLUSION

We have presented an optimal order AMLI method for problems in two-dimensional $H(\text{curl})$ space and three-dimensional $H(\text{div})$ space. In the hierarchical setting, we derived explicit recursion formulae to compute the element matrices, and bounds for the multilevel behavior of γ that are robust with respect to the coefficients in the model problem. The main result of our local analysis (Theorem 3.5) shows that a second order stabilization polynomial (or two inner iterations in nonlinear method), i.e., a W-cycle, is sufficient to stabilize the AMLI process. The presented numerical results, including the case with jumping coefficients (aligned with the coarsest level mesh) confirm the robustness and efficiency of the proposed method. The performance of the presented methods for the range of parameters considered in the paper shows that these methods can be effectively used by the practitioners in the respective fields.

Acknowledgements. The author is very grateful to Dr. Johannes Kraus (RICAM, Linz) for insightful discussions on AMLI methods. Thanks are also due to Dr. Christoph Koutschan (RICAM, Linz) for helpful discussions in proving Lemma 3.4.

APPENDIX A. COEFFICIENTS OF POLYNOMIAL q

In this appendix, we briefly discuss the computation of the polynomial coefficients for linear AMLI W -cycle. In [8, pp. 1582-83], authors provided the explicit formulae for the computation of the coefficients of the polynomial q_ν , for polynomial degrees $\nu = 2, 3$. Note that q_ν is a polynomial of degree $\nu - 1$. Since only the W -cycle is used in this paper, we discuss only the $\nu = 2$ case, i.e. $q(x) = q_0 + q_1x$. Given the constants γ and b (which measures the quality of approximation of A_{11} by C_{11}), the Algorithm 5 computes the coefficients q_0 and q_1 .

Algorithm 5 Coefficients of $q(x)$, see [8, pp. 1582-1583]

$$\begin{aligned} T_2(x) &= 2x^2 - 1 \\ \alpha &= (3 - 4\gamma^2) / \left(1 + 2b + \sqrt{3 - 4\gamma^2 + (1 + 2b)^2}\right) \\ a &= (1 + \alpha) / (1 - \alpha), \quad c = 1 / (1 + T_2(a)) \\ q_0 &= 8ac / (1 - \alpha), \quad q_1 = -8c / (1 - \alpha)^2. \end{aligned}$$

To simplify the expressions, we introduce a variable $s = \sqrt{1 - \gamma^2 + b + b^2}$, which gives $1 - \gamma^2 = s^2 - b - b^2$. Now

$$\begin{aligned} \alpha &= \frac{3 - 4\gamma^2}{1 + 2b + \sqrt{3 - 4\gamma^2 + (1 + 2b)^2}} = \frac{4(1 - \gamma^2) - 1}{1 + 2b + \sqrt{4(1 - \gamma^2) + 4(b + b^2)}} \\ &= \frac{4(s^2 - b - b^2) - 1}{1 + 2b + 2s} = \frac{4s^2 - (1 + 2b)^2}{1 + 2b + 2s} = 2s - 2b - 1. \end{aligned}$$

Therefore, $1 + \alpha = 2s - 2b$. From the relations of a and c , we have $a(1 - \alpha) = 1 + \alpha = 2s - 2b$, and $c = 1/(2a^2)$. Using these simplifications, we get

$$\begin{aligned} q_0 &= \frac{8ac}{1 - \alpha} = \frac{4}{a(1 - \alpha)} = \frac{2}{s - b}, \\ q_1 &= -\frac{8c}{(1 - \alpha)^2} = -\frac{4}{a^2(1 - \alpha)^2} = -\frac{1}{(s - b)^2}. \end{aligned}$$

Therefore, we can write the steps of Algorithm 5 in simplified form as follows:

$$(A.1) \quad s = \sqrt{1 - \gamma^2 + b + b^2}, \quad q_0 = \frac{2}{s - b}, \quad q_1 = -\frac{1}{(s - b)^2}.$$

Note that, in several practical applications, see e.g., [16, 17, 25], the choice of $b = 0$, which yields $q_0 = 2/\sqrt{1 - \gamma^2}$ and $q_1 = -1/(1 - \gamma^2)$, has been used. However, it is observed from the results in this paper that small negative values for b can outperform the results for $b = 0$.

REFERENCES

- [1] Arnold DN, Boffi D, Falk RS. Quadrilateral $H(\text{div})$ finite elements. *SIAM J. Numer. Anal.*, 2005; **42**(6):2429–2451.
- [2] Arnold DN, Falk RS, Winther R. Preconditioning in $H(\text{div})$ and applications. *Math. Comp.*, 1997; **66**:957–984.
- [3] Arnold DN, Falk RS, Winther R. Multigrid in $H(\text{div})$ and $H(\text{curl})$. *Numer. Math.*, 2000; **85**:197–217.
- [4] Axelsson O. Stabilization of algebraic multilevel iteration methods; additive methods. *Numer. Algorithms*, 1999; **21**:23–47.
- [5] Axelsson O, Gustafsson I. Preconditioning and two-level multigrid methods of arbitrary degree of approximations. *Math. Comp.*, 1983; **40**:219–242.
- [6] Axelsson O, Padiy A. On the additive version of the algebraic multilevel preconditioning method for anisotropic elliptic problems. *SIAM J. Sci. Comput.*, 1999; **20**(5):1807–1830.
- [7] Axelsson O, Vassilevski PS. Algebraic multilevel preconditioning methods I. *Numer. Math.*, 1989; **56**:157–177.
- [8] Axelsson O, Vassilevski PS. Algebraic multilevel preconditioning methods II. *SIAM J. Numer. Anal.*, 1990; **27**:1569–1590.
- [9] Axelsson O, Vassilevski PS. A black box generalized conjugate gradient solver with inner iterations and variable-step preconditioning. *SIAM J. Matrix Anal. Appl.*, 1991; **12**(4):625–644.
- [10] Axelsson O, Vassilevski P. Variable-step multilevel preconditioning methods, I: self-adjoint and positive definite elliptic problems. *Numer. Lin. Alg. Appl.*, 1994; **1**:75–101.

- [11] Blaheta R, Margenov S, Neytcheva M. Uniform estimate of the constant in the strengthened CBS inequality for anisotropic non-conforming FEM systems. *Numer. Lin. Alg. Appl.*, 2004; **11**:309–326.
- [12] Blaheta R, Margenov S, Neytcheva M. Robust optimal multilevel preconditioners for non-conforming finite element systems. *Numer. Lin. Alg. Appl.*, 2005; **12**(5-6):495–514.
- [13] Brenner SC. A multigrid algorithm for the lowest-order Raviart-Thomas mixed triangular finite element method. *SIAM J. Numer. Anal.*, 1992; **29**(3): 647–678.
- [14] Brezzi F, Fortin M. *Mixed and Hybrid Finite Element Methods*. Springer-Verlag, Berlin, 1991.
- [15] Eijkhout V, Vassilevski PS. The role of the strengthened Cauchy-Bunyakowski-Schwarz inequality in multilevel methods. *SIAM Review*, 1991; **33**:405–419.
- [16] Georgiev I, Kraus J, Margenov S. Multilevel preconditioning of rotated bilinear non-conforming FEM problems. *Comput. Math. Appl.*, 2008; **55**:2280–2294.
- [17] Georgiev I, Kraus J, Margenov S. Multilevel algorithm for Rannacher-Turek finite element approximation of 3D elliptic problems. *Computing*, 2008; **82**:217–239.
- [18] Girault V., Raviart P.A. *Finite Element Methods for Navier-Stokes Equations*. Springer-Verlag, 1986.
- [19] Hiptmair R. Multigrid method for $H(\text{div})$ in three dimensions. *Electron. Trans. Numer. Anal.*, 1997; **6**(1):133–152.
- [20] Hiptmair R. Multigrid method for Maxwell’s equations. *SIAM J. Numer. Anal.*, 1998; **36**(1):204–225.
- [21] Hiptmair R, Toselli A. Overlapping Schwarz methods for vector-valued elliptic problems in three dimensions. In *Parallel solution of PDEs*, IMA Volumes in Mathematics and its Applications, Springer-Verlag, Berlin, 1998.
- [22] Hiptmair R, Widmer G, Zou J. Auxiliary space preconditioning in $H_0(\text{curl}, \Omega)$. *Numer. Math.*, 2006; **103**:435–459.
- [23] Hiptmair R, Xu J. Nodal auxiliary space preconditioning in $H(\text{curl})$ and $H(\text{div})$ spaces. *SIAM J. Numer. Anal.*, 2007; **45**(6): 2483–2509.
- [24] Kraus J. An algebraic preconditioning method for M-matrices: linear versus nonlinear multilevel iteration. *Numer. Lin. Alg. Appl.*, 2002; **9**:599–618.
- [25] Kraus J, Margenov S. *Robust Algebraic Multilevel Methods and Algorithms*. Radon Series on Computational and Applied Mathematics, **5**, de Gruyter, Berlin, New York, 2009. ISBN 978-3-11-019365-7.
- [26] Kraus J, Tomar SK. Multilevel preconditioning of two-dimensional elliptic problems discretized by a class of discontinuous Galerkin methods. *SIAM J. Sci. Comput.*, 2008; **30**:684–786.
- [27] Kraus J, Tomar SK. A multilevel method for discontinuous Galerkin approximation of three-dimensional anisotropic elliptic problems. *Numer. Linear Algebra Appl.*, 2008; **15**(5):417–438.
- [28] Kraus J, Tomar SK. Algebraic multilevel iteration method for lowest order Raviart-Thomas space and applications. *Int. J. Numer. Meth. Engng*, 2011; **86**:1175–1196.
- [29] Kraus J, Vassilevski P, Zikatanov, L. Polynomial of best uniform approximation to $1/x$ and smoothing in two-level methods. *Comput. Methods Appl. Math.*, 2012; **12**(4): 448–468.
- [30] Lazarov R, Repin S, Tomar SK. Functional a posteriori error estimates for discontinuous Galerkin approximations of elliptic problems. *Numer. Methods Partial Differential Equations*, **25**, 952–971.
- [31] MATHEMATICA. <http://www.wolfram.com/mathematica>
- [32] MATLAB: The language of technical computing. <http://www.mathworks.com/products/matlab>
- [33] Monk P. *Finite Element Methods for Maxwell’s Equations*. Oxford University Press, 2003.
- [34] Notay Y. Flexible conjugate gradients. *SIAM J. Sci. Comput.*, 2000; **22**(4):1444–1460.
- [35] Notay Y. Robust parameter-free algebraic multilevel preconditioning. *Numer. Lin. Alg. Appl.*, 2002; **9**:409–428.
- [36] Notay Y, Vassilevski PS. Recursive Krylov-based multigrid cycles. *Numer. Linear Algebra Appl.*, 2008; **15**(5):473–487.
- [37] Pasciak JE, Zhao J. Overlapping Schwarz methods in $H(\text{curl})$ on polyhedral domains. *J. Numer. Math.*, 2002; **10**(3):221–234.
- [38] Reitzinger S, Schoeberl J. Algebraic multigrid for edge elements. *Numer. Linear Algebra Appl.*, 2002; **9**:223–238.
- [39] Repin S. *A posteriori estimates for partial differential equations*, Walter de Gruyter, Berlin, 2008.
- [40] Repin S, Tomar SK. Guaranteed and robust error bounds for nonconforming approximations of elliptic problems. *IMA J. Numer. Anal.*, 2011; **31**, 597–615.
- [41] Saad Y. *Iterative Methods for Sparse Linear Systems*. PWS Publishing Company, Boston, 1996.
- [42] Vassilevski PS. Multilevel block factorization preconditioners. Springer, New York, 2008.
- [43] Vassilevski PS, Lazarov RD. Preconditioning mixed finite element saddle-point elliptic problems. *Numer. Lin. Alg. Appl.*, 1996; **3**(1): 1–20.
- [44] Vassilevski PS, Wang, JP. Multilevel iterative methods for mixed finite element discretizations of elliptic problems. *Numer. Math.*, 1992; **63**(4): 503–520.
- [45] Xu J. Iterative methods by space decomposition and subspace correction. *SIAM Rev.*, 1992; **34**(4): 581–613.
- [46] Xu J. The auxiliary space method and optimal multigrid preconditioning techniques for unstructured grids. *Computing*, 1996; **56**: 215–235.
- [47] Xu J, Zikatanov L. The method of alternating projections and the method of subspace corrections in Hilbert space. *J. Amer. Math. Soc.*, 2002; **15**(3): 573–597.